12-2021

Increasing Hydrophilicity and Transparency of Diamond-Like Carbon Thin Films with Dopants for an Anti-Fogging Laparoscope Coating

Anna Bull
University of Tennessee, Knoxville, abull4@vols.utk.edu

To the Graduate Council:

I am submitting herewith a thesis written by Anna Bull entitled "Increasing Hydrophilicity and Transparency of Diamond-Like Carbon Thin Films with Dopants for an Anti-Fogging Laparoscope Coating." I have examined the final electronic copy of this thesis for form and content and recommend that it be accepted in partial fulfillment of the requirements for the degree of Master of Science, with a major in Biomedical Engineering.

<div align="right">

Jacqueline A. Johnson, Major Professor

</div>

We have read this thesis and recommend its acceptance:

Jacqueline A. Johnson, Russell L. Leonard, Trevor M. Moeller

<div align="right">

Accepted for the Council:
<u>Dixie L. Thompson</u>

Vice Provost and Dean of the Graduate School

</div>

(Original signatures are on file with official student records.)

Increasing Hydrophilicity and Transparency of Diamond-Like Carbon Thin Films with Dopants for an Anti-Fogging Laparoscope Coating

A Thesis Presented for the

Master of Science

Degree

The University of Tennessee, Knoxville

Anna Beatrice Bull

December 2021

This thesis is dedicated to my family and friends, especially my parents, who have always encouraged me to do my best. I could not have achieved this goal without their support.

ACKNOWLEDGEMENTS

ABSTRACT

Laparoscopes are prone to fogging, which can lead to a limited field of view during surgical procedures. Current methods of mitigating fogging issues are not efficient or can require costly modifications to the laparoscope. Previous studies of diamond-like carbon (DLC) coatings found doping the films improved hydrophilic qualities, suggesting their possible use as antifogging coatings for laparoscopes. For this work, two series of DLC films, doped with either silicon monoxide (SiO) or aluminum oxide (Al_2O_3) were investigated.

The biocompatibility, transparency, and stability of these films were assessed through cellular assays, spectrophotometry, and simulated body fluid soaking experiments. Contact angle and surface energy measurements were performed to assess the hydrophilic qualities of the films. Plasma cleaning was utilized as a surface treatment to improve hydrophilicity; time-studies were performed to assess the stability of this treatment. Raman spectroscopy, atomic force microscopy, and adhesion tests were performed to assess the chemical, physical, and mechanical characteristics of the films.

The silicon monoxide doped films demonstrated improved transparency and hydrophilic qualities. Samples subjected to plasma cleaning had contact angles under 5° when measured within 60 minutes of treatment. From the time-studies performed, the hydrophilicity of the silicon monoxide doped films was improved for over 24 hours after treatment. The aluminum oxide doped films demonstrated transparency results of up to 97% over the visible spectrum indicating the dopant helped improve transparency. After plasma cleaning, aluminum oxide doped samples demonstrated a contact angle of 8° within 60 minutes of treatment. Both series demonstrated similar biocompatibility results with cellular assay viability values being statistically similar to the control media. No delamination of the films from either series was observed when soaked in simulated body fluid over the course of 40 weeks. The results of this research show promise for DLC as an antifogging coating for laparoscopes.

TABLE OF CONTENTS

LIST OF TABLES

LIST OF FIGURES

INTRODUCTION

Diamond-Like Carbon

Diamond-like carbon (DLC) films have been studied extensively because of their favorable properties such as low-friction, chemical inertness, corrosion resistance, and scratch resistance [1]. DLC films are from a class of amorphous carbon materials with properties like diamond. DLC films are available in different compositions, with or without hydrogen, containing varying amounts of sp^3 hybridized carbon atoms as demonstrated in Figure 1 [2].

Dopants can be added to DLC to modify physical, electrical, and mechanical properties of the films [3-5]. Common dopants include fluorine, boron, silicon, oxygen, and nitrogen [6]. DLC has been employed in a wide range of applications in industry for manufacturing, electronics, optics, medicine, and many more [7]. DLC films have also been used for decorative purposes, including firearms, watches, and sports equipment because of their scratch resistant properties [7].

Interest in DLC films in medicine is growing because of their previously mentioned properties and because of their biocompatibility [8]. They have applications in orthopedic, cardiovascular, and dental industries [8]. For orthopedic applications, studies have demonstrated that DLC can reduce wear and particle generation in load bearing implants such as coating femoral heads for in hip replacement procedures [9]. DLC was found to significantly reduce platelet activation and thrombosis on coated stents in clinical testing [10]. Additional research has found doping DLC with fluorine resulted in antibacterial properties of the film [11].

Previously completed DLC research at the University of Tennessee Space Institute found that SiO doped films maintained transparency and demonstrated improved hydrophilic properties [12]. This previous research showed that SiO doped DLC films have the potential to become anti-fogging coatings, specifically for the prevention of fogging and contamination on lenses used for guided surgical procedures. In this work, the effects of plasma surface treatments and alternative dopants for DLC films were investigated. In addition, the DLC films were tested for biocompatibility and biostability.

Pulsed Laser Deposition

Pulsed laser deposition (PLD) is a method of depositing thin films established in the mid-1960s after the invention of the pulsed ruby laser [13]. In the 1980s, PLD was used in the development of superconductive materials which demonstrated improved quality over films synthesized using other methods [13]. Since then, the development of improved laser technology has led to PLD becoming a competitive method of thin film growth for a variety of applications, including for optical coatings and superconducting thin films [13, 14]. PLD is experimentally and conceptually straightforward; however, it is remarkable, as it can deposit a wide variety of materials [13]. Figure 2 is a simplified illustration of the PLD process. PLD is a physical vapor deposition method where a pulsed laser is focused through an optical window of a vacuum chamber where it strikes a target material. The material is then vaporized from the target, forming a plume which grows perpendicular to the surface [15]. This plume condenses on a substrate resulting in film growth.

The growth of the film depends on several parameters during the deposition including, but not limited to, laser energy, substrate material and temperature, background pressure, and distance from target to substrate [14]. PLD has advantages over other deposition methods because of its ability to make thin films out of numerous forms of solid matter [15]. The process is simple, parameters can quickly be adjusted, and it can be used to deposit a multi-component film utilizing different targets [15]. Finally, the ability to deposit in different atmospheres allows for doping, compound formation of films, or even textured nanoparticles [16, 17].

PLD is not without some limitations in commercial and experimental applications. For some materials during the ablation process, molten particles or fragments are present in the deposited film which significantly reduces film quality [15]. PLD has not proven feasible for large scale commercial applications because of the localized area where the film is deposited [15].

Camera Guided Laparoscopy

Camera guided laparoscopy is a surgical technique which allows for a surgeon to image the inside of the abdomen without the need for open surgery. The rod lens camera system allows for real time imaging of the abdomen and pelvis which can be useful for gallbladder removal, endometriosis diagnosis, and other surgical procedures [18]. Because of the smaller incision sites from the laparoscope and associated tools, this procedure is minimally invasive and leads to reduced recovery time [19]. One disadvantage of laparoscopic procedures is the camera is prone to fogging and contamination during surgery [20, 21]. This leads to a reduced surgical field of view, which may necessitate removal of the lens for cleaning, leading to increased surgery time and greater risk of infection, which can cause higher costs for the patient and poorer outcomes [22, 23].

Current methods to reduce fogging include the use of anti-fogging gels and solutions on the lens, wiping of the lens during procedures, CO_2 insufflation, interoperative heating of the laparoscope, and preheating via water baths [21-25]. These methods are often temporary, costly, and/or require removal of the laparoscope from the body [21-23]. Gels and solutions often require re-application during the procedure [21-23]. Removal and re-insertion of the laparoscope is time-consuming and increases the length of surgical procedures which is costly; however, this can also lead to increased risk of surgical site infections. Laparoscope heating requires modification to the laparoscope which can be costly [24, 25]. CO_2 insufflation and warming baths have not proven to provide significant reduction of fogging [24].

To reduce fogging of the laparoscope, it is necessary to develop a coating for the laparoscope that is hydrophilic, maintains transparency, has strong adhesion to glass, is biostable, and biocompatible. Hydrophilicity is important, as the low contact angle properties of the film allows water droplets which can form beads on the laparoscope to flatten out into one smooth layer, reducing light scattering [21-23]. Figure 3 illustrates the difference between a hydrophilic substrate and an untreated substrate. This research covers the suitability of doped DLC films for antifogging laparoscope applications.

2
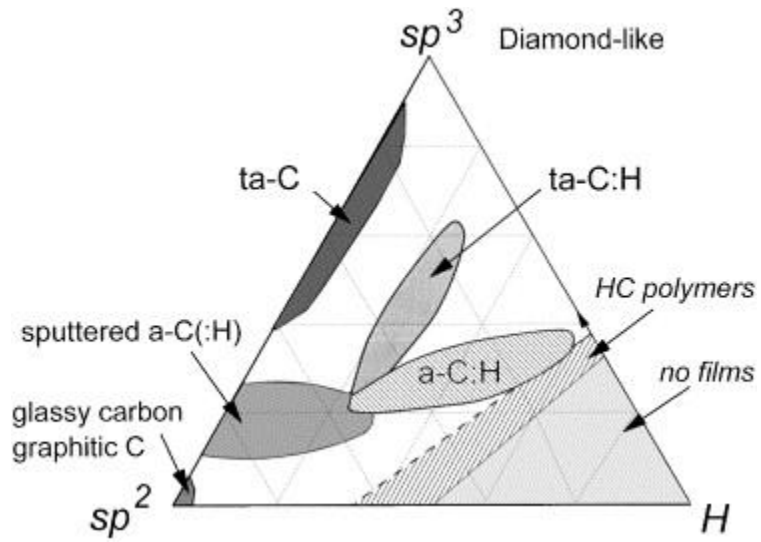
Figure 1. Ternary Phase Diagram of DLC. Used with permission [2].
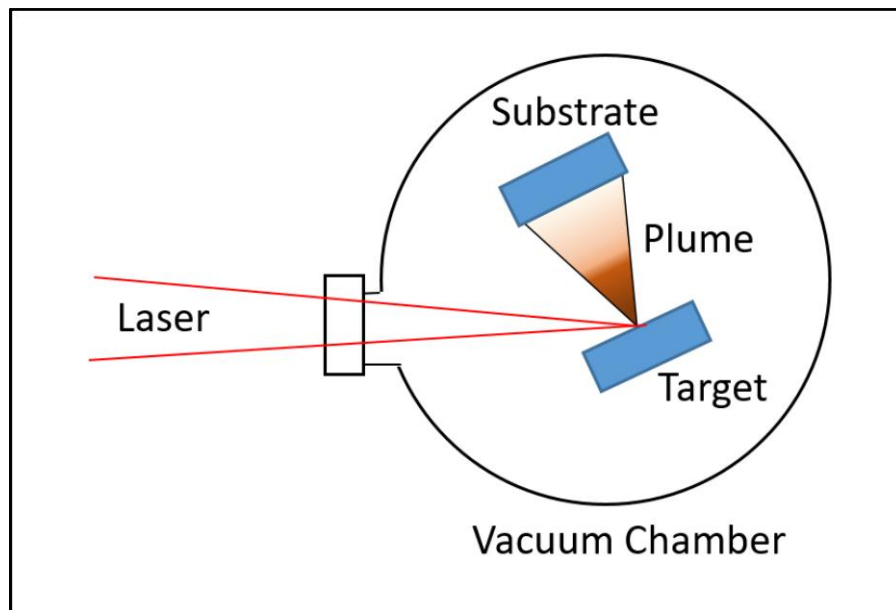
Figure 2. Schematic Diagram of Pulsed Laser Deposition System.
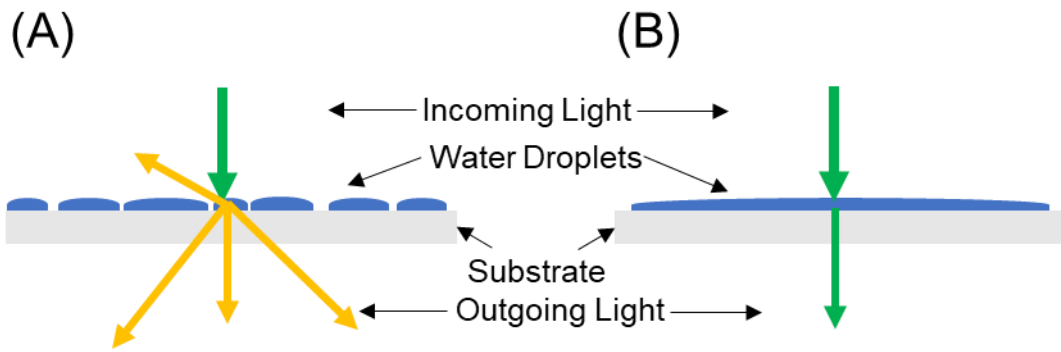
Figure 3. Light Passing Through Two Different Materials: (A) Untreated Glass, (B) Hydrophilic Glass.

CHAPTER I:
Evaluation of the Stability and Biocompatibility of Antifogging SiO Doped Diamond-Like Carbon Coatings

Abstract

Current laparoscopes suffer from fogging and contamination difficulties, resulting in a reduced field of view during surgery. Intraoperative cleaning of the laparoscopic lens is time-consuming and can increase the likelihood of surgical site infections. In previous studies, diamond-like carbon (DLC) coatings, doped with SiO, have demonstrated hydrophilic properties. The authors hypothesized that an SiO-doped DLC coating would mitigate the fogging and fouling issues associated with laparoscopic lenses and eliminate the need for intra-operative cleaning; the scratch-resistant nature of DLC would provide additional benefits. For this study, a series of DLC films doped with SiO were produced by pulsed laser deposition for the purpose of biocompatibility and stability testing. Multiple depositions were performed utilizing varying percentages of dopant to observe the effects of SiO content on the hydrophilicity, transparency, and biocompatibility of the films. The deposited films are transparent, although they have a brown tint. DLC films doped with SiO demonstrated improved hydrophilic capabilities with contact angles being reduced from 70° to under 40°. Samples were subjected to plasma cleaning and found to have significantly improved contact angle results with values under 5° after treatment, a significant reduction on the originally measured 33.3°. Time-studies were performed to determine the stability of the films' hydrophilic nature, both as-made and after plasma cleaning, with the treated films maintaining an average contact angle of 5° for over 24 hours. The biocompatibility of these films was analyzed through CellTiter-Glo assays and simulated-body fluid soaks to determine the suitability of these films as a coating for surgical instruments. The films demonstrated statistically similar levels of cell viability when compared to the control media. The SiO doped films displayed improved transparency levels in comparison to undoped films achieving up to an average of 80% transmission over the visible spectrum. These SiO doped DLC films show promise as a method of fog prevention for laparoscopes due to their decreased contact angles, transparency, biostability, and biocompatibility. These results could be utilized in other antifogging applications where transparency is key for design success.

Introduction

Since the introduction of camera guided laparoscopy, the number of laparoscopic procedures performed has increased each year. Laparoscopic procedures have been found to result in increased patient comfort and decreased mortality rates than with open surgical procedures [19]. One drawback to these procedures is the susceptibility of the lens to fogging [20]. Fogging can lead to reduced surgical field of view requiring intraoperative cleaning which may require repeated removal and reinsertion of the laparoscopic lens; this process can lead to longer surgery times and greater risk of surgical site infection [21-23]. Some methods of reducing fogging of lenses involve the use of a surfactant to reduce the surface tension of the liquids interacting with the lens [21-23]. These surfactants often need reapplication during the procedure requiring removal of the laparoscope from the body, increasing the risk of contamination. Insufflation, which uses CO_2 gas to inflate the abdomen during the procedure, and water baths have been investigated for the

6

reduction of fogging, with limited data to support their effectiveness [24]. Other methods require extensive modification to the lens, such as the addition of a heating mechanism to the end of the laparoscope, which can be costly and still leave the lens susceptible to fogging [24, 25].

Diamond-like carbon (DLC) films are from a class of amorphous materials composed of a mixture of sp^2 and sp^3 hybridized carbons [26]. DLC demonstrates corrosion and scratch resistance, chemical inertness, and a low friction coefficient [27]. DLC can be modified for a wide variety of applications as the ratio of sp^3 and sp^2 hybridization of the film affects the structure and properties of DLC coatings. Additionally, it can be doped with other elements to improve specific properties [3-5].

DLC films are growing in recognition as a material that can be used to of improve medical devices. DLC has been investigated as a coating in replacement hip, shoulder, and knee joints [9]. These films are not prone to corrosion and have demonstrated good biocompatibility in blood contacting-devices [10].

DLC films are of interest in antifogging applications for camera guided medical scopes because their properties can be tuned with dopants to improve hydrophilicity and transparency. Medical scopes are critical in the diagnosis and treatment for a wide variety of health conditions. There are different forms of scopes utilized depending on the medical procedure including bronchoscopes, otoscopes, laparoscopes, and many more.

This manuscript presents a continuation of research completed by Leonard et al. involving silicon monoxide (SiO) doped DLC films [12]. A series of DLC films doped with SiO was produced through pulsed laser deposition and evaluated through biocompatibility and stability testing, this series utilized greater amounts of SiO dopant than the previously completed research. The effect of plasma cleaning on the hydrophilic characteristics of the films was investigated. The longevity of their hydrophilicity was determined via time studies. Biostability and biocompatibility of the films were explored through simulated body fluid tests and cellular assays.

Materials and Methods

DLC films were deposited on UV grade Corning 7980 fused silica substrates, with thicknesses of 500 μm. Each sample deposition coated three 25 × 25 mm substrates and one 38 × 38 mm substrate. An illustration of the substrates attached to the sample holder is shown in Figure 4. Physical and optical characterizations were performed on the 25 × 25 mm substrates while the 38 × 38 mm piece was set aside for biocompatibility testing. Before deposition, the substrates were ultrasonically cleaned in acetone and methanol for ten minutes each. They were rinsed with ultrapure water and dried with compressed nitrogen following sonication, then placed in a 1:1 (v:v) piranha solution (H_2SO_4 (99.99%) and H_2O_2 (30%)) soak for 2 minutes. The final cleaning steps were a soak in ultrapure water for 1 minute plus rinse and drying with compressed nitrogen before being fixed on the sample holder.

The thin film samples were synthesized through pulsed laser deposition (PLD) with a 193 nm ArF excimer laser. An image of the PLD system can be seen in Figure A1 in the appendix. The laser pulse repetition rate was 100 Hz at a laser energy of 5.0 mJ resulting in a laser fluence of 4.1 J/cm^2 based on a 0.06 mm^2 spot size. For all samples, the deposition chamber pressure remained under 3.0×10^{-6} Torr. A multicomponent PLD target was made consisting of semiconductor-grade graphite (Poco Graphite, Inc.) and SiO (Kurt J. Lesker Co.) as shown in Figure 5. Axial target movement is controlled by a programmable stepper motor, so that the position can be manipulated to alter the portion of the multicomponent target that the laser strikes.

Six DLC samples were synthesized with differing amounts of SiO dopant. The samples were synthesized with 400,000 total laser pulses with the amount of laser pulses on the dopant ranging from 0 – 30%. Table 1 details the number of laser pulses on each material for the respective sample. A separate sample set was made with the same process parameters as the 30% SiO doped sample on four, 25 × 25 mm substrates for additional optical characterization. Samples were stored in ambient air when not being characterized.

Tape tests were performed to assess film adhesion to the substrate following the methods dictated by ASTM D3359. These tests were performed with Adhesive ASTM D3359 Cross-Hatch Adhesion Test Tape (Elcometer 99). The samples and tape were examined visually for any signs of delamination.

The effects of differing SiO dopant amounts on the optical transmission of the samples were determined by spectrophotometry. The transmission spectra were measured from 200 nm to 900 nm at 1.0 nm increments with a GenTech Scientific TU-1901 spectrophotometer. The data was collected with a PC equipped with UVWin5.0 software. An uncoated fused silica substrate was used as a reference during each measurement. Witness marks present on the deposited substrates ensured the position of the measured area was consistent between samples.

Contact angle of the films was measured with a Krüss DSA20E Easy Drop Standard equipped with a software-controlled system of dosing. The probe liquids tested were ultrapure water, with a resistivity of 12.6 MΩ·cm or greater, and benzyl alcohol (Sigma-Aldrich) both with a drop volume of 2μL per measurement. Five measurements were performed on each sample with both probe liquids. The water contact angle was assessed on as-made samples and samples subject to plasma cleaning. Benzyl alcohol contact angles were measured on the as-made samples and used for surface energy calculations with the Fowkes method [28]. The Fowkes method calculates surface energy, using contact angle results from two probe liquids, as a sum of the dispersive and polar components as shown below in equation 1 [29].

$$\gamma_s = \gamma_s^d + \gamma_s^p \ (1)$$

The thicknesses of the films were determined with a J.A. Woollam M-2000VI ellipsometer. The data was collected with a Windows XP computer equipped with CompleteEASE software.

Experiments in simulated body fluid (SBF) were conducted to assess the biostability of the films. The sample deposited on the 38 × 38 mm substrate was cut into twelve 8.45 × 8.45 mm pieces to ensure they were properly sized for a close fit in a welled cell culture plate and to remove the masked portions of the sample. This allowed for multiple tests to be completed and for uniformity of the exposed film/substrate interface for all specimens. These pieces were then cleaned in accordance with their method of testing. For SBF soaks, the samples were cleaned by sonication in ultrapure water and then methanol. The SBF was made following the methods established by Cho et al., 1995 [30]. The soaks were performed and kept at body temperature of 37° C in a Lauda Ecocline E100 Immersion Thermostat water bath and assessed every 4 weeks for 48 weeks via an optical microscope. For SBF soaks, each of the doped films were scored before insertion. This allowed the assessment of any changes in the interface between the DLC and fused silica during soaking.

CellTiter-Glo assays were performed to assess the effects of DLC films on cell viability. The samples were cleaned in ultrapure water by sonication. NIH/3T3 cells (ATCC stock no: CRL-1658) were used for evaluation of cell viability. NIH/3T3 cells were cultured according to ATCC recommendations in Dulbecco's Modified Eagle's Medium grown with 10% iron supplemented bovine calf serum and penicillin/streptomycin. All cultures were grown in T-75 flasks (ThermoFisher Scientific) at 80% confluence or less. NIH/3T3 cells were seeded in standard 24-well plates at 25,000 cells/well in 1mL media containing DLC films and cultured for 24 hrs. The

films were sterilized with 70% ethanol after fabrication, washed with 1x phosphate buffered saline (PBS) to remove residual ethanol, and positioned coated-side-up in 24-well plates before seeding with NIH/3T3 cells. Samples were maintained under sterile cell culture conditions for 24 hrs. A modified commercial CellTiter-Glo (Promega) assay was carried out to evaluate cell viability at the end of the culture period and the resulting luminescence was assessed via IVIS. At the conclusion of the 24-hour incubation period, 24-well plates were allowed to equilibrate to room temperature for 30 minutes. Before being mixed with an orbital shaker for 2 minutes, 600 μL of media was removed from each well and 400 μL of CellTiter-Glo reagent was then added directly to the media in each well. Once mixing was complete, the 24-well plates were allowed to rest for 10 minutes before 100 μL samples of the resulting solution was transferred to black-walled 96-well plates for analysis in order to eliminate any interference caused by the DLC films during IVIS imaging. The average viability of NIH/3T3 cells grown on DLC films was normalized to media controls. An assay of 1% T-x-100 treated NIH/3T3 cells served as a control to simulate complete cytotoxicity. Note that the testing of the 100% carbon, the 15% SiO doped, and 20% SiO doped samples were performed on a different day than the 10%, 25% and 30% SiO doped samples.

The effects of plasma cleaning on the hydrophilicity of the films was investigated with a Harrick Plasma PDC-32G benchtop plasma cleaner with an argon processing gas. The films were subjected to 3 minutes of treatment at medium RF power before being removed for contact angle testing. The contact angles of two 30% SiO doped samples were tested, and the sample subjected to plasma cleaning was measured within 60 minutes of being treated.

A study was conducted to determine the stability of the samples' contact angle, both as made and after plasma cleaning. The contact angle for each sample was measured in 24-hour intervals over the course of 14 days; additional measurements, at greater frequency, were taken at the early stage of testing. The films were stored in air for the duration of the time study.

Atomic force microscopy (AFM) was performed to determine the film morphology and roughness on both as-made films and a plasma cleaned film. The plasma cleaned film was characterized within 12 hours of being treated. The measurements were performed with a Bruker Dimension Icon Atomic Force Microscope connected to a computer equipped with ScanAsyst software in contact mode. A 2 μm × 2 μm sample area with a scanning speed of 10 μm/s at a resolution of 256 × 256 pixels was collected. The data were analyzed on a separate computer with NanoScope Analysis V1.2.0 software installed.

Raman Spectroscopy was performed with a Thermo Scientific DXR Raman Microscope, and the data was collected through Omnic Spectra Software. The laser wavelength was 532 nm and was focused through an X50 objective lens at a power of 10 mW. All acquisitions were for 10 seconds with 20 accumulations taken at each measured location. Gaussian deconvolution of the peaks was performed using Origin software.

Results & Discussion

Representative samples of the as-made films are shown in Figure 6. The films are transparent and show no signs of delamination or other defects as seen from visual inspection. No delamination of the films was observed after performing tape tests, demonstrating the effective adhesion of the films to the substrate. The 100% carbon sample was noticeably darker than the SiO doped samples. However, the samples become increasingly darker as the amount of SiO dopant is increased.
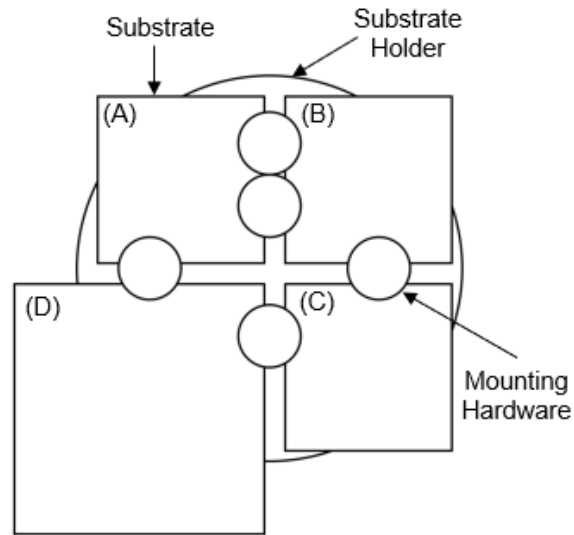
Figure 4. Schematic of the Substrate Holder with Samples Attached. Note: The mounting hardware results in "witness marks" on the sample substrates.
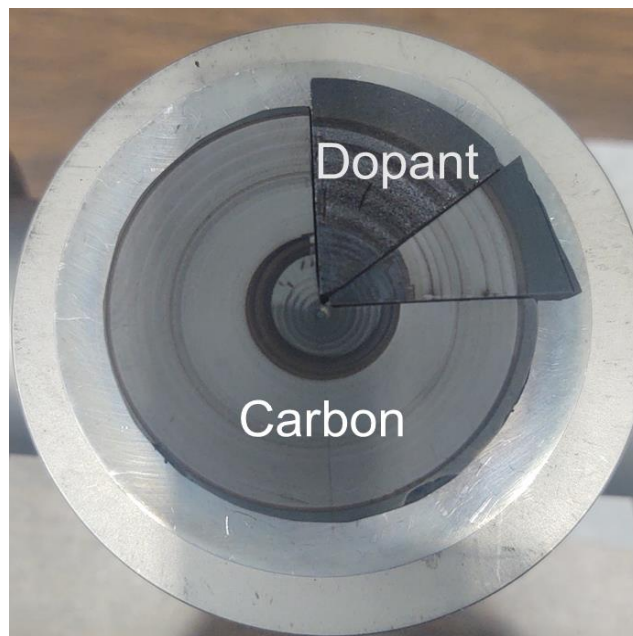
Figure 5. Multi-component SiO Doped Target.

Table 1. Doped and Undoped DLC Deposition Parameters.

Sample Name	Pulses on SiO Dopant (%)	Pulses on Carbon	Pulses on SiO Dopant
ABB025	None	400000	N/A
ABB007	10	360000	40000
ABB008	15	340000	60000
ABB009	20	320000	80000
ABB010	25	300000	100000
ABB012	30	280000	120000
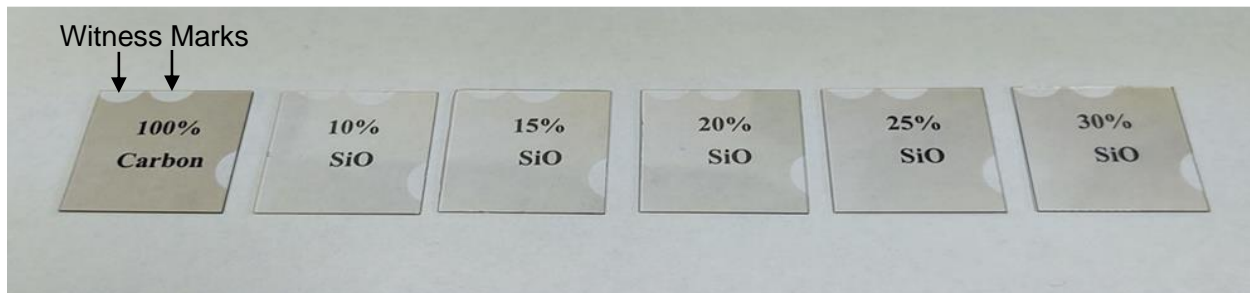
Figure 6. Undoped and Silicon Monoxide Doped DLC Samples. Note: Witness marks associated with the mounting hardware used during deposition can be seen in the upper left and bottom right of the samples. For each sample, identifying text can be seen through the film and substrate.

The effects of SiO dopant amount on film transparency can be seen in Figure 7. The shape of the transmission spectrum for the undoped DLC film is markedly different from the rest of the samples; it has increased transmission at the lower energy region of the spectrum and decreased transmission in the higher energy (blue and ultraviolet) regions. In general, the transparency of the doped films decreased with increasing SiO content. Through the visible spectrum, the 10% SiO doped sample had the highest measured transmission. The initial increase in the film transparency is likely due to the reduced amount of carbon in the film. Silicon has been shown to increase the sp^3 hybridization of DLC films, making them more transparent, which follows the observed trend of the experimental series [1]. The hypothesis is the doped films get darker with increasing SiO content due to the incorporation of SiO particles into the matrix; SiO is a dark brown, opaque material. Finally, the thickness of the films has a direct effect on the transmittance results and in how the films absorb light. This was explored through calculating the attenuation coefficient of the films at a wavelength of 450 nm. These results, shown in Figure 8, were calculated by following the methods by Manjunatha & Paul using the Beer-Lambert Law [31]. From these calculations it was determined that increasing the amount of dopant in the films increased the attenuation coefficient values. However, the values for the doped samples are much smaller than the undoped carbon sample.

The water contact angle results from the as-made films are shown in Figure 9. It was observed that the addition of SiO as a dopant significantly lowered the contact angle, which is in agreement with Leonard et al [12]. The quantity of SiO was also observed to affect the contact angle with the 30% SiO doped sample having a contact angle almost 20° lower than the 10% SiO doped sample. The influence of SiO content on the contact angle decreases between 15% and 30% SiO as there was only a 4° difference between these samples. This suggests that the upper limit of SiO dopants' ability to increase hydrophilicity is in the 15 - 30% range.

Increased surface energies are known to correspond to decreased contact angles and the effects of increasing SiO dopant on surface energy are shown in Figure 10. The highest measured surface energy was just over 80 mN/m for the 30% SiO doped sample while the undoped sample had a surface energy of 41 mN/m. The difference in surface energy values of the undoped and doped samples demonstrates that the SiO dopant helped improve the hydrophilicity of DLC, which agrees with the results collected during contact angle measurements. Although the hydrophilicity of the films increased with increasing SiO content, the transparency of the films decreased demonstrating a trade-off between transparency and hydrophilicity. The 15% SiO doped sample could be the most effective composition for antifog coating applications as it provided a balance of decreased contact angle with limited loss in transparency.

The SiO doped films were significantly thicker than the undoped film, as shown in Table 2. The difference is likely due to the variation in ablation rate between the two target materials, graphite and SiO, with the ablation rate of SiO being much greater. This could be due to the formation of larger particulates during the ablation of the SiO wedge, this was explored through AFM. SiO may have a higher ablation rate than graphite because of its lower density which could result in an increased growth rate and target degradation [32].

The difference in contact angle between an as-made sample and a plasma cleaned sample can be observed in Figure 11. An angle of less than 5° was observed for the plasma cleaned sample (Figure 11(A)), which is significantly less than the original 33.3° measured on the untreated films (Figure 11(B)). These results show that plasma cleaning may be an effective way to enhance the antifogging properties of the material and reverse the increase in contact angle that occurs over time due to surface contamination. Furthermore, plasma cleaning would have the additional benefit of sterilizing the instrument, as required before surgical procedures [33].
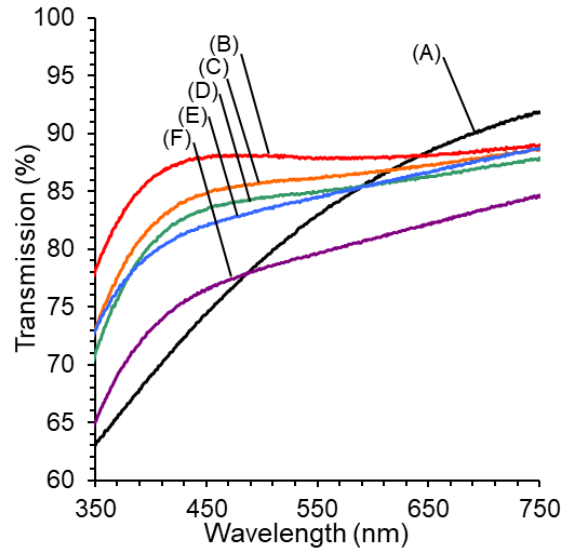
Figure 7. Transmission Spectra of DLC Films Composed of Varying Amounts of Silicon Monoxide Dopant: (A) 100% Carbon, (B) 10% Dopant, (C) 15% Dopant, (D) 20% Dopant, (E) 25% Dopant, and (F) 30% Dopant.
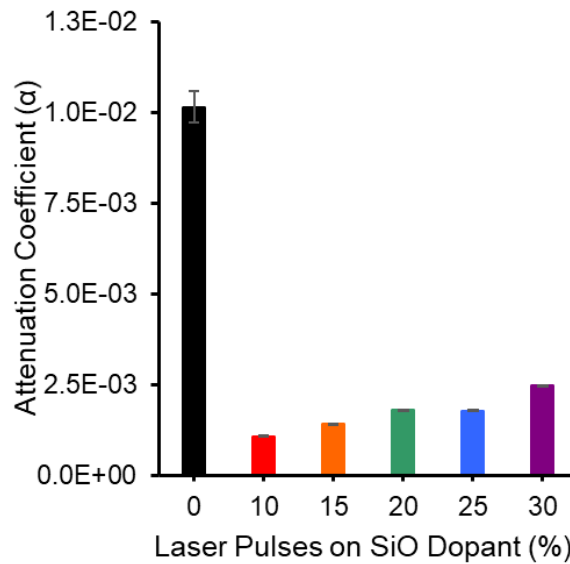
Figure 8. Attenuation Coefficient of DLC Films Composed of Varying Amounts Laser Pulses on Silicon Monoxide Dopant at 450 nm. Note: Error bars are present but difficult to observe for each sample.

13
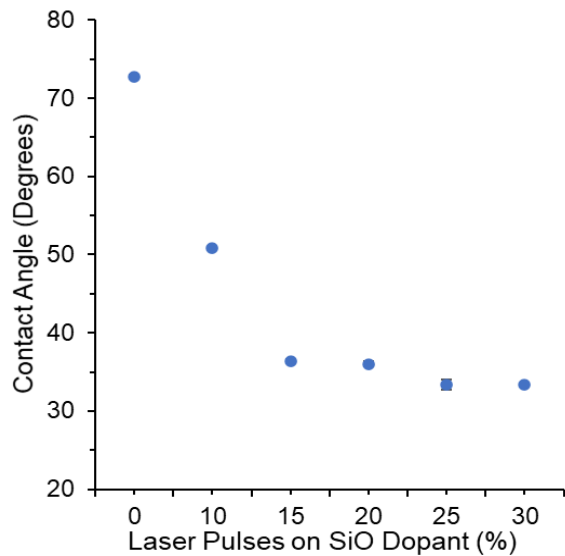
Figure 9. The Effect of Silicon Monoxide Dopant on Average Water Contact Angle. Note: Error bars are present but difficult to observe for each sample.
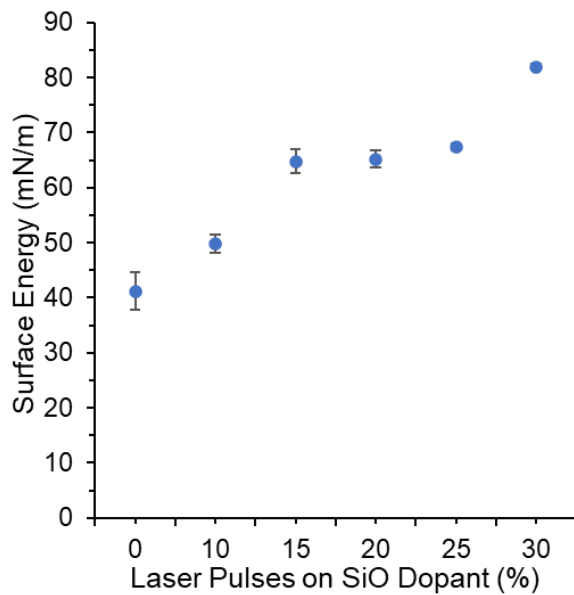
Figure 10. The Effect of Silicon Monoxide Dopant on Average Surface Energy. Note: Error bars are present but difficult to observe for each sample.

Table 2. Thicknesses of the SiO Doped Films as a Function of Laser Pulses.

Sample Name	Pulses on Dopant (%)	Thickness (nm)
ABB025	None	29 ± 2
ABB007	10	112 ± 2
ABB008	15	115 ± 2
ABB009	20	101 ± 1
ABB010	25	111 ± 1
ABB012	30	108 ± 1
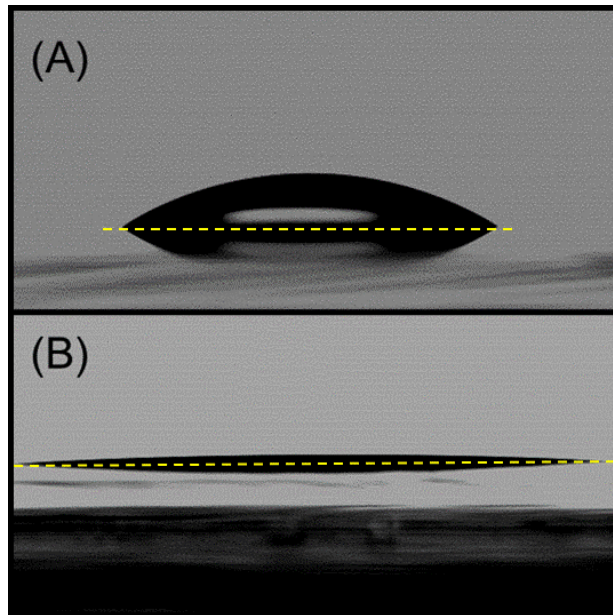
Figure 11. Profile of Water Drops on 30% SiO Doped Samples: (A) An As-made Film and (B) 60 minutes after treatment. Note: The baseline for each measurement is indicated with a yellow, dashed line.

Time study results for an as-made and a plasma cleaned film are shown in Figure 12. Conducting contact angle measurements over 14 days allowed for observation of the longevity of the plasma cleaning treatment effect on the films. The plasma cleaned films began at an average angle of 5° that was sustained for 24 hours. After two days, the contact angle measurements of the films rose to over 20° and for the duration of the study slowly rose to just under 30° by the fourteenth day of observation. This is a significant improvement on the as-made sample which maintained an average contact angle of 33° for the duration of the time study. Two weeks after the time-studies completion, the contact angle for the treated film was measured and it had returned to ~33°. The decrease and subsequent increase in contact angle may be caused by the formation of hydroxyl free radicals in the film surface as detailed by Subedi et al, where they observed the same trend of increasing contact angle after a few hours of treatment [34]. Alternatively the increase in contact angle of the plasma cleaned films could also be due to hydrocarbons and other contaminants attaching to the film surface while in ambient air [35].

The Raman spectra of the undoped and doped films can be observed in Figure 13. The sp^2/sp^3 ratio of DLC dictates the overall properties of the films [36, 37]. The D peak, resulting from carbon-carbon bond stretching and contractions, is at ~1360 cm^{-1} and the G peak, caused by in plane stretching of carbon-carbon bonds, is at ~1580 cm^{-1} [37]. The ratio of the intensity of the D and G peak (I_D/I_G) can give insight into the size and number of sp^2 clusters within the DLC films [37]. The G peak characteristics of these films are shown in Table 3. The shift in G peak in the doped samples, along with the increased I_D/I_G ratio, suggest a greater sp^2 content in these films. This generalization does not hold true for the 10% SiO doped sample which demonstrated a much smaller I_D/I_G ratio than the other doped samples. The decrease could indicate a reduction in aromatic cluster formation or an increase in sp^3 clusters. The peaks at ~1060 cm^{-1} and 1200 cm^{-1} can be attributed to the fused silica substrate [38, 39].

The morphology and roughness of a plasma cleaned film, as-made films, and an uncoated substrate were investigated by AFM. The AFM results and root mean square (RMS) roughness are demonstrated in Figures 14 and 15. The AFM results for the undoped sample (Figure 14(B)) demonstrated a much smoother film than the as-made SiO doped film (Figure 14(C)). This increase in roughness can be attributed to the formation of particulates of SiO during the ablation process. There are repeated bands visible in the uncoated fused silica substrate (Figure 14(A)) resulting from its fabrication; these also can be seen in the undoped and SiO doped samples. This likely affects the roughness of the undoped sample but not as much on the SiO doped sample because of the particulates. The plasma cleaned sample (Figure 14(D)) had a different topography than the as-made sample. This could mean the plasma cleaning process not only removed contaminants but also caused an etching effect on the film resulting in a film more textured in appearance.

Figure 16 shows a 15% SiO doped sample. In Figure 16(A) there is no delamination present before insertion. After 48 weeks of soaking, as shown in Figure 16(B), there is still no delamination or significant changes in the film. The lack of changes after soaking helps verify the stability of the film.

Figure 17 shows the results of acute toxicity of DLC films evaluated ex vivo 24 hours after incubation of NIH/3T3 cells with DLC films made with various SiO dopant levels. Compared to the media, the DLC films all had statistically similar levels of cell viability observed among all coatings. These results helped demonstrate the biocompatibility of DLC films. Additional studies should be performed on the plasma cleaned films as the biocompatibility of those films was not investigated. Though this would be helpful for understanding how the treated films interact with the body, it could prove challenging because of the 24-hour time point restriction before the effects begin to wear off.

Figure 12. Results of Average Contact Angle Measurements of Plasma Cleaned vs. As-Made Films over 14-Days: (A) As-made and (B) Plasma Cleaned. Note: Error Bars are present but are not always visible for each measurement.
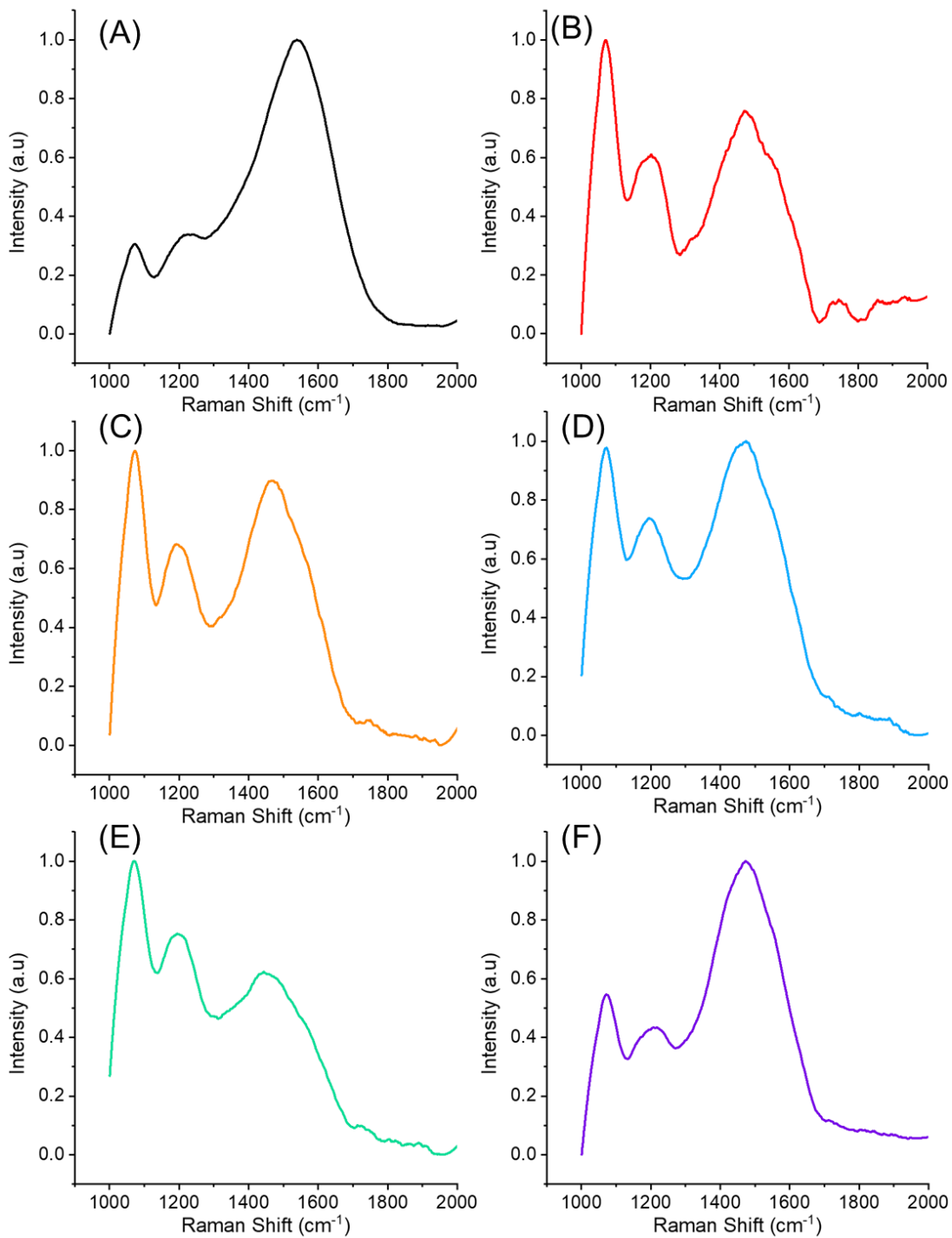
Figure 13. Raman Spectra of DLC Films with Varying Amounts of Laser Pulses on Silicon Monoxide Dopant: (A) 100% Carbon, (B) 10% Dopant, (C) 15% Dopant, (D) 20% Dopant, (E) 25% Dopant, and (F) 30% Dopant. Note: This data has been normalized.
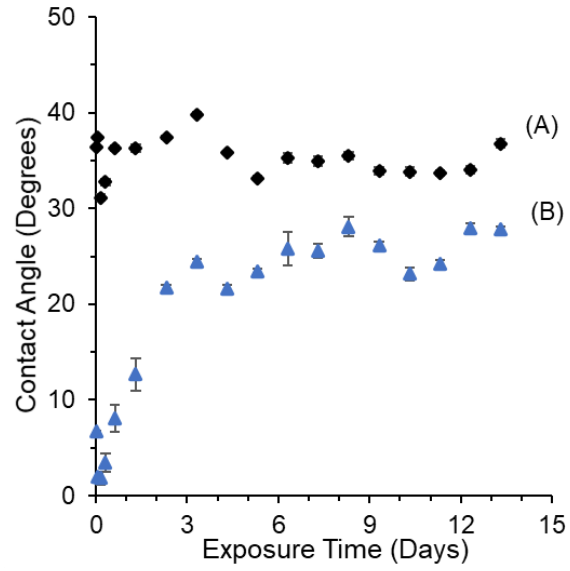
18

Table 3. Gaussian Fitting of Raman Spectra of Undoped and SiO Doped DLC Films.

Sample Name	Pulses on Dopant (%)	G Peak Position	I_D/I_G	Full Width Half Maximum G Peak
ABB025	None	1548 ± 1	0.4 ± 0.02	266 ± 3
ABB007	10	1471 ± 6	0.3 ± 0.01	194 ± 1
ABB008	15	1473 ± 2	0.5 ± 0.02	245 ± 2
ABB009	20	1467 ± 2	0.6 ± 0.20	297 ± 2
ABB010	25	1452 ± 3	0.8 ± 0.01	303 ± 1
ABB012	30	1477 ± 5	0.5 ± 0.03	239 ± 3
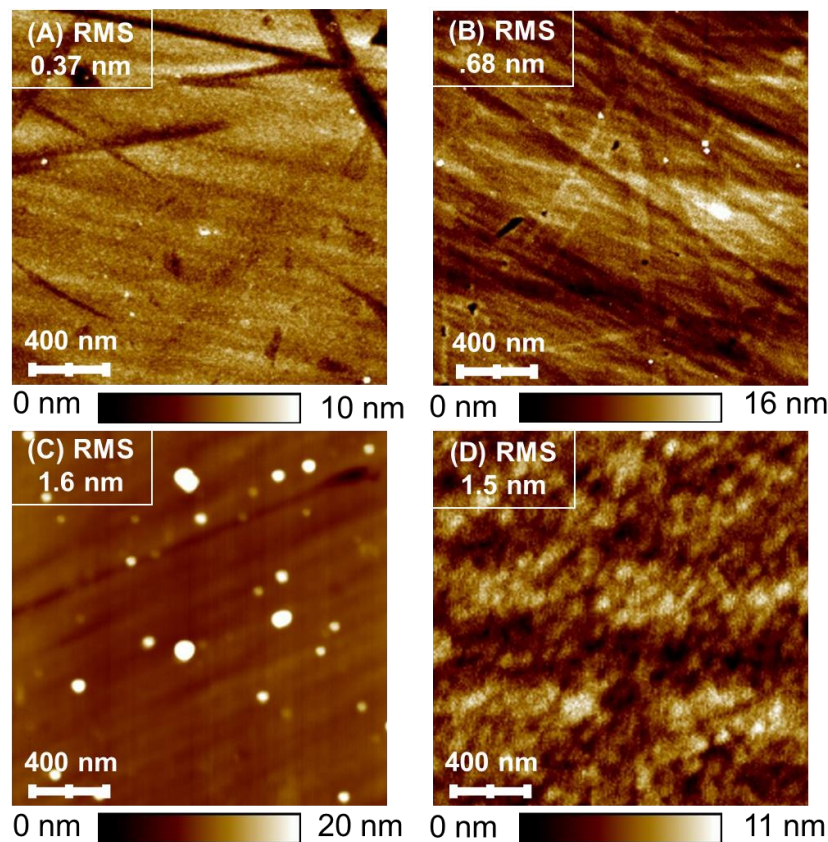
Figure 14. Representative AFM Images of DLC with Varied Dopant Amounts and an Uncoated Substrate: (A) Uncoated Substrate; (B) 100% Carbon; (C) 30% SiO Dopant; (D) Plasma Cleaned 30% SiO Dopant.
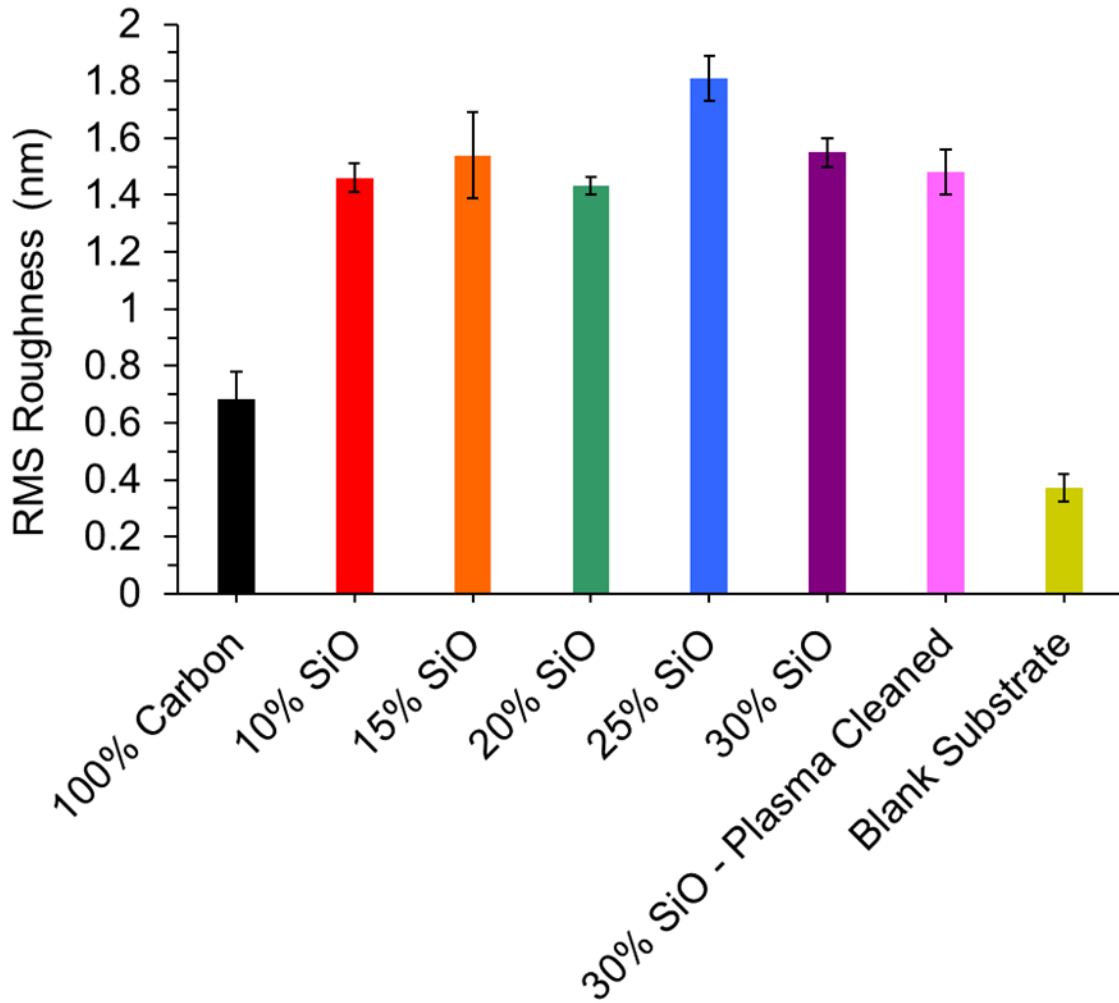
Figure 15. RMS Roughness Results for an Uncoated Substrate, DLC with Varied SiO Dopant Amounts, and a Plasma Cleaned Film.
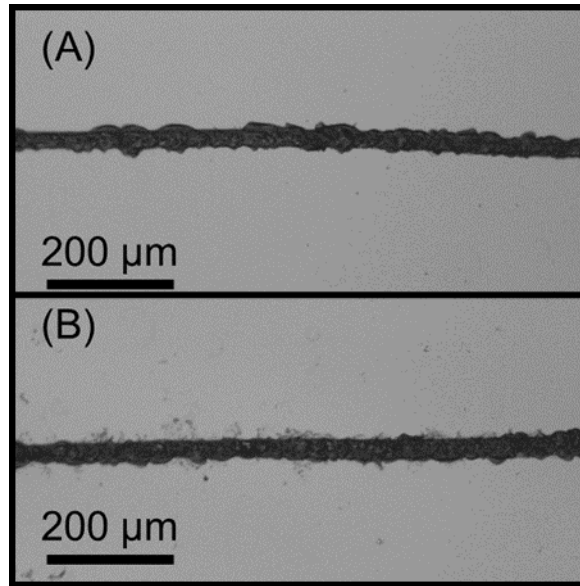
Figure 16. Photographs of a 15% SiO Doped DLC Sample: (A) Before Soaking and (B) After Soaking in SBF for 48 weeks.
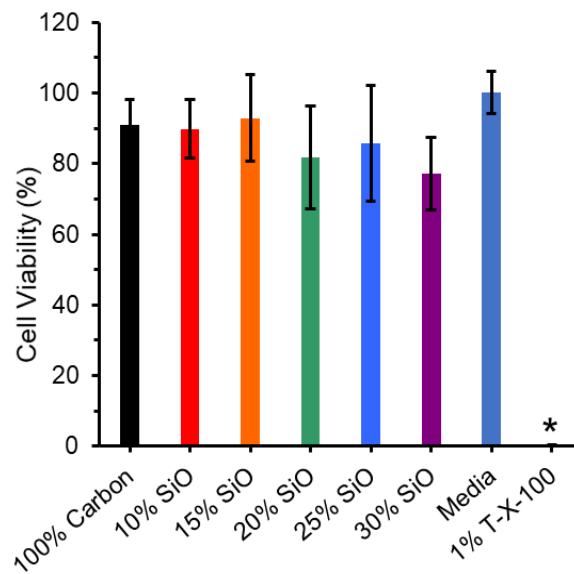
Figure 17. Average Viability Normalized to Media Controls of NIH 3T3 Cells Incubated for 24 Hours with Various SiO Doped DLC Films (n = 5 Technical Replicates). The significance of the data was evaluated via ordinary one-way ANOVA with Dunnett's Multiple Comparison Test (*$p < 0.05$).

Conclusion

Diamond-like carbon thin films doped with varying amounts of SiO were synthesized via pulsed laser deposition on fused silica substrates. Spectrophotometry showed that the incorporation of SiO improved transparency of the films. The stability of the films was maintained while soaked in simulated body fluid stored at 36.5° C for 47 weeks. Plasma cleaning reduced surface roughness and decreased contact angle to 5° for over 24 hours in the doped films. In vitro cell viability assays found all the films demonstrated similar biocompatibility results to the media control with no loss in cell viability. The findings of this research study demonstrate the possibility of using SiO doped DLC as an antifogging coating for a laparoscopic lens.

CHAPTER II:
Evaluation of the Transparency and Biocompatibility of Al_2O_3 Doped Diamond-Like Carbon Thin Films

Abstract

Laparoscopes and other camera guided medical scopes suffer from fogging and contamination difficulties. This causes a reduced field of view during surgery and intraoperative cleaning of the laparoscopic lens can lead to increased surgery time and greater risk of surgical site infections. In previous studies, utilizing a dopant in diamond-like carbon (DLC) coatings resulted in improved hydrophilic properties. This study investigates the use of aluminum oxide (Al_2O_3) as a dopant in DLC films for antifogging applications. A series of DLC films doped with Al_2O_3 were produced by pulsed laser deposition. Varying percentages of dopant were tested to observe the effect of content on the hydrophilicity, transparency, and biocompatibility of the films. The doped films demonstrated improved transparency over the visible spectrum. Samples that were plasma cleaned were found to have significantly improved contact angle results with values under 8°. The biocompatibility of these films was analyzed with CellTiter-Glo assays and simulated body fluid soaks to determine the suitability of these films as a coating for surgical instruments. The films demonstrated statistically similar levels of cell viability when compared to the control media. Due to the instability of the contact angles of these doped films they are not suitable for antifogging applications. However, their high transparency, biocompatibility, and biostability could make them useful for biomedical applications where a transparent coating is necessary.

Introduction

The first successful endoscopes were developed to help image the inside of the body in the mid-1800s by Spaner and Warnock [40]. Because of technological advances in the 1960s, cameras were then incorporated into the endoscope system [40]. Since then, they have become a popular surgical tool for doctors to remove gallstones, gastrointestinal disease diagnosis, and more [18]. Additionally, they are utilized in robotic surgical systems [41, 42]. Their introduction has led to reduced recovery time in comparison to open surgery [19]. One limitation is that they are prone to fogging, which can lead to reduced visibility. Fogging can lead to reduced surgical field of view requiring intraoperative cleaning which may require repeated removal and reinsertion of the laparoscopic lens; this process can increase surgery time, risk of error during the procedure, or elevated risk of surgical site infection [20, 21]. Current antifogging methods utilize surfactants to reduce the ability of liquids interacting with the scope to bead up, which can cause light scattering [21-23]. The surfactant is not permanent and often requires reapplication due to procedure length. A permanently hydrophilic coating applied to the lens surface could mitigate this problem. Diamond-like carbon (DLC) thin films could be a potential method of solving this problem due to their versatility.

DLC films have been researched extensively as protective coatings in biomedical devices because of their wear resistance, chemical inertness, low friction coefficient, and bioinertness [43]. DLC is from a class of amorphous carbon materials with properties like diamond due to the presence of a high number of sp^3 bonds [43]. Dopants can be used in combination with DLC to enhance specific properties of the films, reduce internal stresses, which can cause poor adhesion to the substrate, and are important for furthering the use of DLC in biomedical applications [6].

24

Common dopants include F, SiO, and Ti to improve antibacterial, hydrophilic, and mechanical characteristics of DLC respectively [6, 44].

Aluminum oxide (Al_2O_3), more widely known as alumina, is the most commonly occurring oxide of aluminum. It is the second hardest naturally occurring material available and is being researched in biomedical applications extensively because of its high hardness, wear resistance, and chemical stability [45]. It has previously been investigated for use in protective coatings for biomedical devices and joint replacements [46-48]. It is of interest as a dopant in DLC to raise the amount of oxygen in the films to promote increased hydrogen bonding [12].

In this work, Al_2O_3 doped DLC films synthesized via pulsed laser deposition (PLD) were evaluated for use as an antifogging biocompatible coating. The physical and optical characteristics of these films were characterized by Raman spectroscopy, atomic force microscopy, energy-dispersive X-ray analysis, contact angle measurements, and spectrophotometry. The biocompatibility of the films was tested with cell viability assays and the biostability tested through simulated body fluid (SBF) soaks.

Materials and Methods

Films were deposited on UV grade Corning 7980 fused silica substrates, 500 μm thick. Each sample deposition coated three 25 × 25 mm substrates and one 38 × 38 mm substrate. Physical and optical characterizations were performed on the 25 × 25 mm substrates while the 38 × 38 mm piece was set aside for biocompatibility testing. Before deposition, the substrates were ultrasonically cleaned in acetone and methanol for ten minutes each. They were rinsed with ultrapure water and dried with compressed nitrogen following sonication. Following this, they were then placed in a in a 1:1 (v:v) piranha solution (H_2SO_4 (99.99%) & H_2O_2 (30%)) soak for 2 minutes. The final cleaning steps were a soak in ultrapure water for 1 minute plus rinse and drying with compressed nitrogen before being fixed on the sample holder.

Pulsed laser deposition (PLD) was used to synthesize thin film samples. A 193 nm ArF excimer laser was used in all depositions. An image of the PLD system can be seen in Figure A1 in the appendix. The laser pulse repetition rate was 100 Hz, and the laser fluence was 4.1 J/cm^2 based on a 0.06 mm^2 spot size. For all samples, the deposition chamber pressure remained under 2.9×10^{-6} Torr. A multicomponent PLD target was made consisting of semiconductor-grade graphite (Poco Graphite, Inc.) and Al_2O_3 (Kurt J. Lesker Co.) as shown in Figure 18. Axial rotation of the target is controlled by a programmable stepper motor, so that the position can be manipulated to alter the portion of the multicomponent target that the laser strikes.

Six DLC samples were synthesized with differing amounts of Al_2O_3 dopant but the same number of laser pulses. The samples were grown using 400,000 total laser pulses with the amount of laser pulses on the dopant ranging from 0 – 25%. Table 4 details the number of laser pulses on each material for the respective sample. A separate sample set was made with the same process parameters as the 17.5% Al_2O_3 doped sample on four, 25 × 25 mm substrates for additional optical characterization. Two additional 17.5% Al_2O_3 doped samples were made with 2,400,000 and 4,800,000 laser pulses respectively to determine the effects of thickness on transparency.

The effect of differing Al_2O_3 dopant amounts on the optical transmission of the samples was determined by spectrophotometry. The transmission spectra were measured from 200 nm to 900 nm at 1.0 nm increments with a GenTech Scientific TU-1901 spectrophotometer. The data was collected with a PC equipped with UVWin5.0 software. An uncoated fused silica substrate acted

as a reference during each measurement. Witness marks present on the deposited substrates ensured the position of the measured area was consistent.

Tape tests were performed to assess film adhesion to the substrate following the methods dictated by ASTM D3359. These tests were performed with Adhesive ASTM D3359 Cross-Hatch Adhesion Test Tape (Elcometer 99). The samples and tape were examined visually for any signs of delamination.

Contact angle of the films was measured with a Krüss DSA20E Easy Drop Standard equipped with a software-controlled system of dosing. The probe liquids tested were ultrapure water, with a resistivity of 12.6 MΩ·cm or greater, and benzyl alcohol (Sigma-Aldrich) both with a drop volume of 2µL per measurement. Five measurements were performed on each sample with both probe liquids. The water contact angle was assessed on as-made samples and samples subject to plasma cleaning. Benzyl alcohol contact angles were measured on the as-made samples and used for surface energy calculations with the Fowkes method [28]. The Fowkes method calculates surface energy, using contact angle results from two probe liquids, as a sum of the dispersive and polar components as shown below in equation 1 [29].

$$\gamma_s = \gamma_s^d + \gamma_s^p \ (1)$$

Film thickness was measured by stylus profilometry by measuring the step height of the witness marks present on each sample. The data was collected with a Veeco Dektak 150 Surface Profiler equipped with a diamond-tipped stylus. The measurements began on the masked portion of the substrate and moved to the top of the film during the scan. The scan length was 2000 µm with a measurement time of 120 seconds allowing for a resolution of 0.014 µm for each sample.

Experiments in simulated body fluid (SBF) were conducted to assess the biostability of the films. The sample deposited on the 38 × 38 mm substrate was cut into twelve 8.45 × 8.45 mm pieces to ensure they were properly sized for a close fit in a welled cell culture plate and to remove the masked portions of the sample. This allowed for multiple tests to be completed and for uniformity of the exposed film/substrate interface for all specimens. These pieces were then cleaned in accordance with their method of testing. For SBF soaks, the samples were cleaned by sonication in ultrapure water and then methanol. The SBF was made following the methods established by Cho et al., 1995 [30]. The soaks were performed at 37 °C, which is human body temperature, using a Lauda Ecocline E100 Immersion Thermostat water bath and assessed every 4 weeks for 40 weeks via an optical microscope. Each of the films were scored before insertion into the SBF. Scoring the films allowed for the assessment of any changes at the interface between the films and fused silica during soaking.

CellTiter-Glo assays were performed to assess the effects of DLC films on cell viability. The samples were cleaned in ultrapure water by sonication. NIH/3T3 cells (ATCC stock no: CRL-1658) were used for evaluation of cell viability. NIH/3T3 cells were cultured according to ATCC recommendations in Dulbecco's Modified Eagle's Medium supplemented with 10% iron supplemented bovine calf serum and penicillin/streptomycin. All cultures were grown in T-75 flasks (ThermoFisher Scientific) at 80% confluence or less. NIH/3T3 cells were seeded in standard 24-well plates at 25,000 cells/well in 1mL media containing DLC films and cultured for 24 hrs. The films were sterilized with 70% ethanol after fabrication, washed with 1x PBS to remove residual ethanol, and positioned coated-side-up in 24-well plates before seeding with NIH/3T3 cells. Samples were maintained under sterile cell culture conditions for 24 hrs. A modified commercial CellTiter-Glo (Promega) assay was carried out to evaluate cell viability at the end of the culture period and the resulting luminescence was assessed via IVIS. At the conclusion of the 24-hour incubation period, 24-well plates were allowed to equilibrate to room temperature for 30 minutes. Before mixing with an orbital shaker for 2 minutes, 600 µL of media was removed from each well and 400 µL of CellTiter-Glo reagent was then added directly to the media in each well.

Once mixing was complete, the 24-well plates were allowed to rest for 10 minutes before 100 μL samples of the resulting solution was transferred to black-walled 96-well plates for analysis to eliminate any interference caused by the DLC films during IVIS imaging. The average viability of NIH/3T3 cells grown on DLC films was normalized to media controls. An assay of 1% T-x-100 treated NIH/3T3 cells served as a control to simulate complete cytotoxicity.

A Harrick Plasma PDC-32G benchtop plasma cleaner with argon gas was used to investigate the effects of plasma cleaning on the hydrophilicity of the films. The films were subjected to 3 minutes of treatment at medium RF power before being removed for contact angle testing. Two 17.5% Al_2O_3 doped samples were tested, and the plasma cleaned sample was measured within 60 minutes of being treated.

A study was conducted to determine the stability of the samples' contact angle, both as-made and after plasma cleaning. The contact angle for each sample was measured in 24-hour intervals over the course of 14 days; additional measurements, at greater frequency, were taken in the early stages of testing.

Atomic force microscopy (AFM) was performed to determine the film morphology and roughness on both as-made films and a plasma cleaned film. The plasma cleaned film was characterized within 12 hours of being treated. The measurements were collected with a Bruker Dimension Icon Atomic Force Microscope connected to a computer equipped with ScanAsyst software in contact mode. A 2 μm × 2 μm sample area with a scanning speed of 10 μm/s at a resolution of 256 × 256 pixels was collected. The data was analyzed on a separate computer with NanoScope Analysis V1.2.0 software installed.

Raman Spectroscopy was performed using a Thermo Scientific DXR Raman Microscope and the data was collected with Omnic Spectra Software. The laser wavelength was 532 nm and was focused through a ×50 objective lens at a power of 10 mW. All acquisitions were for 10 seconds with 20 accumulations taken at each measured location. Gaussian Deconvolution of the peaks was performed using Origin software.

Results and Discussion

Representative samples of the as-made Al_2O_3 doped films are shown in Figure 19. The films are transparent and show no signs of delamination or defects from visual inspection. No delamination of the films was observed after performing tape tests, demonstrating the effective adhesion of the films to the substrate. The undoped carbon sample was noticeably darker than any of the Al_2O_3 doped samples. The Al_2O_3 doped films did demonstrate a slight brown tint at the lowest dopant level, but this coloring was nearly imperceptible at the higher dopant levels.

The effects of Al_2O_3 dopant on film transparency can be observed in Figure 20. The undoped DLC sample demonstrated significantly reduced transmission properties in comparison to the doped samples. The transparency in the Al_2O_3 doped films increased with increasing dopant levels up to 17.5% before beginning to decrease at the greater dopant levels. Because film thickness can have a significant effect on transparency, the attenuation coefficient for each film was calculated at 450 nm wavelength to allow direct comparison of the films. The thickness of the doped films ranged from ~18-26 nm as shown in Table 5. The attenuation coefficients of each of the films, shown in Figure 21, were calculated following the methods of Manjunatha & Paul, using the Beer-Lambert Law [31]. The changes in transparency may also be attributed to particulates present in the films from the Al_2O_3 or carbon. Particle size and distribution can affect light scattering as the particulates act as defects or scattering locations in Al_2O_3 and can determine if a film will be

transparent, translucent, or opaque [49]. Alternatively, in research that utilized Al_2O_3 as a transparent coating for electrodes, it was determined that metallic aluminum was opaque due to its plasma reflection of free electrons and used it in the fabrication of the Al_2O_3 for that study [50].

Longer depositions of the 17.5% Al_2O_3 doped film were performed to determine if the films would maintain their high transparency at greater thicknesses. The transmission results of the 1, 6, and 12-hour long depositions over the visible spectrum (380 nm – 750 nm) were 98.7%, 97.1%, and 96.0% respectively. The spectrophotometer results agreed with the thickness measurements and the transparency of the films decreased with longer deposition times. The attenuation coefficient at 450 nm wavelength and thickness of the three 17.5% Al_2O_3 films can be seen in Figure 22. As expected, the larger quantity of pulses caused more material to be ablated from the target ensuing a thicker film. This increased thickness helps ensure less uncertainty in the attenuation coefficient calculations of the films. There was only a 10% difference in the attenuation coefficient values of the 12 hour and the 1-hour depositions, helping confirm the values calculated for the thin films produced with the shorter deposition time.

The effects of aluminum oxide on contact angle varied widely depending on the dopant amount present in the films. The initial trend of the films was a decrease in water contact angle as shown in Figure 23. However, when the dopant amount reached 20% the contact angle experienced a sharp increase, rising from 32° to just over 60°. This indicated that the upper limit to reduce contact angle was 17.5% dopant levels. Surface energy testing was performed to better understand these results.

The surface energies of the films should be the inverse of the contact angle results as increased surface energies are known to correspond to decreased contact angle. The surface energy of the Al_2O_3 doped films followed this expected trend as shown in Figure 24. The highest measured surface energy of the doped films was 70 mN/m for the 17.5% Al_2O_3 doped sample and the lowest was 41 mN/m for the 25% Al_2O_3 doped film. This was as expected and the surface energy results indicate that an Al_2O_3 dopant can help increase the hydrophilicity of the DLC films, but only to a certain point. The polar and dispersive forces of these surface energy results are useful for better understanding the wettability of the films. While the total surface energy is important, the polar and dispersive forces may give more insight into the differences in wettability. A study by Wang et al. found that increased polar forces in doped DLC films resulted in decreased contact angles [51]. As the amount of dopant in the films increases the polar forces decrease which may have contributed to the increase in contact angle for the Al_2O_3 doped films.

The difference in contact angle from an as made and plasma cleaned sample can be observed in Figure 25. Two 17.5% Al_2O_3 doped samples were tested. The plasma cleaned sample was measured within 60 minutes of treatment. A contact angle of less than 8° was observed in comparison to the original 32° measured on the untreated films. This indicated that plasma cleaning the films could be an effective method of treatment immediately before a surgical procedure to improve the anti-fogging capabilities of the film.

The plasma cleaned film had an average contact angle of 8° within the first 2 hours of treatment as shown in Figure 26. However, within the first 48 hours the contact angle of this film rose to over 50°. Over the remainder of the time-study, both the treated and as-made sample experienced a significant increase in their contact angle. By the final day of observation, they both had contact angles of ~90°. The initial decrease in contact angle may have been caused by the formation of hydroxyl free radicals in the film surface as detailed by Subedi et al [34]. The significant increase in contact angle of both films is likely due to airborne contamination from hydrocarbons and other contaminants sticking to the film surface from ambient air [35]. Overall, these results

demonstrated that argon plasma cleaning is not a promising method of surface treatment to significantly increase hydrophilicity long term.

No delamination or significant structural changes occurred during the 40 weeks of soaking in SBF on the undoped or doped films. Figure 27 shows a 10% doped sample where there is no delamination before (Figure 27(A)) or after (Figure 27(B)) insertion into the SBF. The absence of change in the films after soaking verifies their stability.

The acute toxicity of Al_2O_3 doped DLC films were evaluated ex vivo, 24 hours after incubation of NIH/3T3 cells, these results can be observed in Figure 28. The results of the cell viability assays were statistically similar between the films and the control media. This test helped demonstrate the biocompatibility of DLC films.

Representative images of the morphology for doped and undoped samples can be observed in Figure 29. The blank substrate (Figure 29(A)) appears smooth and the striations across the sample are a result of the manufacturing process. These same striations are observed on the undoped sample (Figure 29(B)) and additional particulates are present on the surface. The 17.5% doped sample (Figure 29(C)) has small rounded particulates on the surface giving it a more textured appearance than the other three films. These particulates could be observed in all of the doped films and varied in size depending on dopant levels. Plasma cleaning the 17.5% doped film (Figure 29(D)) appears to have removed the small particulates observed in the as made samples. This may mean the power level of the plasma cleaner was too high during treatment and subsequently etched away the surface material during the cleaning process. Perhaps lowering the power level or reducing the cleaning time for this process might prevent the removal of material, while still allowing for contact angle reduction.

The root mean square (RMS) roughness of each of the films can be observed in Figure 30. There was little change of the surface roughness of the undoped DLC film and the substrate. Although there was a significant increase in surface roughness when the dopant was incorporated. In general, there was a gradual decrease in surface roughness with increased doping; however, the 20% doped sample was an anomaly. A few factors may have contributed to variations in roughness: a change in the area of the target that was ablated during synthesis and the target condition. The reduction in roughness could be due to a reduction in particulate size, allowing for improved film uniformity; however, additional characterization of these films is needed to better understand how the dopant affects surface roughness.

Because of poor signal to noise ratio in the Raman spectra at greater dopant levels, due to how thin the films were, a representative doped sample was used for comparison to the undoped carbon film, shown in Figure 31. The Raman spectra were deconvoluted using a Gaussian function for the D and G peaks. The D peak, resulting from carbon-carbon bond stretching and contractions, is at ~1360 cm^{-1} and the G peak, caused by in plane stretching of carbon-carbon bonds, is at ~1580 cm^{-1} [37]. While the G peak position remained close to ~1580 cm^{-1}, the D peak made a small shift down towards 1320 cm^{-1} after incorporating the dopant. The increase in the I_D/I_G ratio of the doped film demonstrated an increase in the graphitic nature of the DLC film as shown in Table 6. The undoped carbon sample had 3 distinct peaks over the spectrum which can be attributed to carbon oxygen bonding at ~1050 cm^{-1}, the fused silica substrate at ~1200 cm^{-1}, and a large broad peak due to the overlapped G and D peaks mentioned previously [52]. The doped samples had up to 7 peaks over the same range. A majority of these peaks can be attributed to substrate interference during spectrum collection, such as the three additional peaks in the 10% doped DLC sample, located at ~1715, 1810, and 1890 cm^{-1}. The same peaks were observed in the Raman spectra of an uncoated substrate.
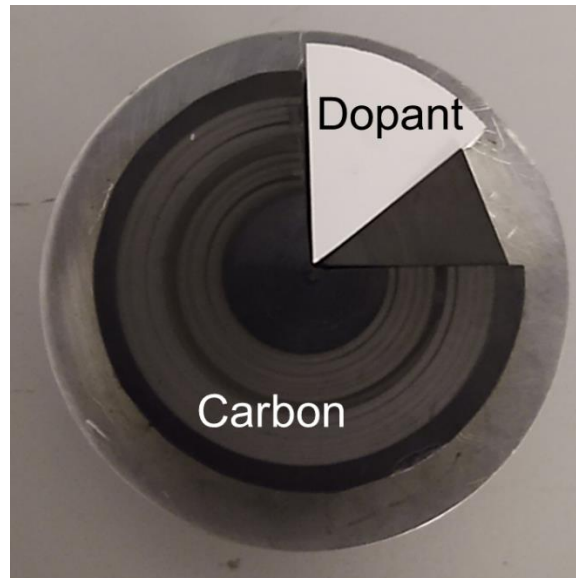
Figure 18. Multi-Component Al$_2$O$_3$ Doped Target.

Table 4. Parameters of DLC Films with Varied Amounts of Al$_2$O$_3$ Dopant.

Sample Name	Pulses on Dopant (%)	Pulses on Carbon	Pulses on SiO
ABB025	N/A	400000	N/A
ABB019	10	360000	40000
ABB020	15	340000	60000
ABB023	17.5	330000	70000
ABB021	20	320000	80000
ABB022	25	300000	100000
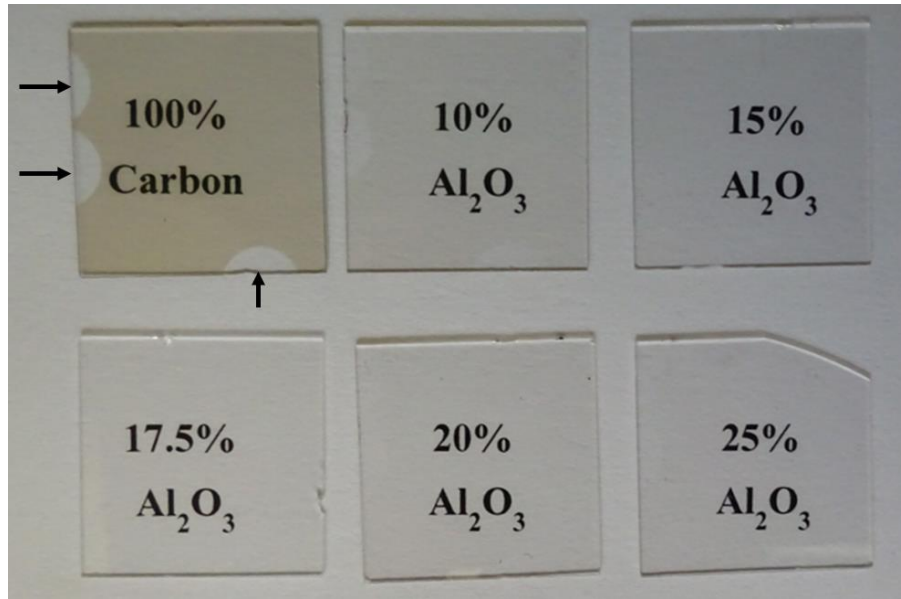
Figure 19. Undoped and Aluminum Oxide Doped DLC Samples. Note: Witness marks from the mounting hardware used during deposition can be observed on the samples as indicated by arrows on the 100% carbon sample. The text behind the samples serves as an illustration of the film's transparent qualities.
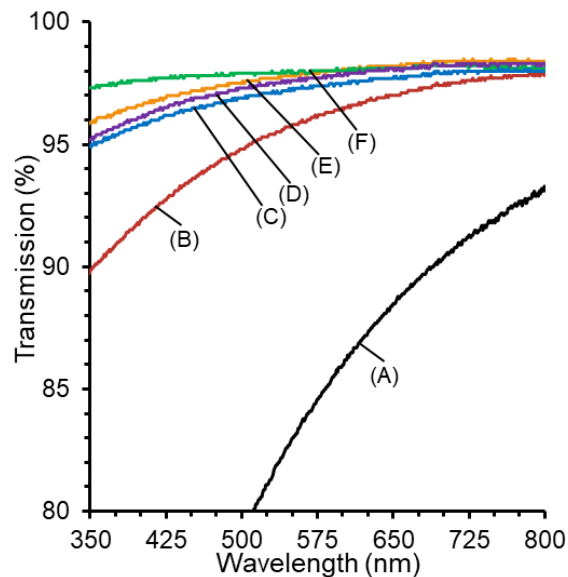
Figure 20. Transmission spectra of DLC Films with Varied Amounts Laser Pulses on Al₂O₃ Dopant. (A) 100% Carbon, (B) 10% Dopant, (C) 15% Dopant, (D) 17.5% Dopant, (E) 20% Dopant, and (F) 25% Dopant.

Table 5. The Effects of Varied Aluminum Oxide Dopant Amount on Film Thickness.

Sample Name	Total Pulses	Pulses on Dopant (%)	Thickness (nm)
ABB025	400,000	None	35.6
ABB019	400,000	10	24.1
ABB020	400,000	15	18.3
ABB023	400,000	17.5	19.4
ABB021	400,000	20	23.4
ABB022	400,000	25	25.8
ABB048	2,400,000	17.5	50.2
ABB046	4,800,000	17.5	70.9
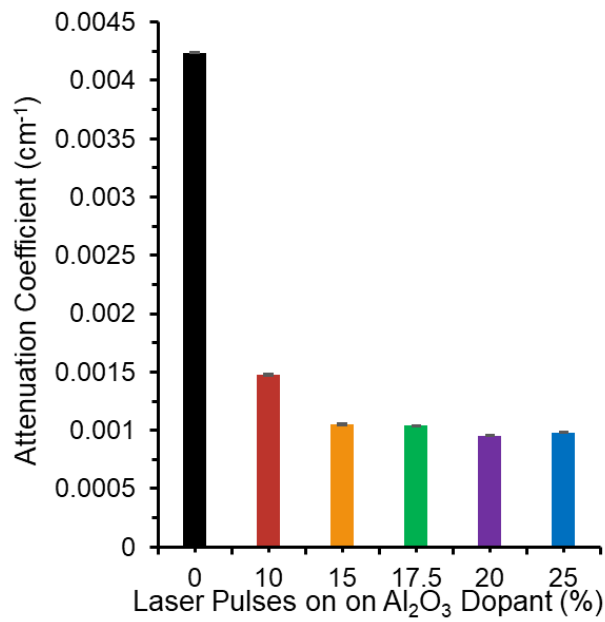
Figure 21. Attenuation Coefficient of Al$_2$O$_3$ Doped DLC Films Made with 400,000 Total Laser Pulses. Note: Error bars are present but difficult to observe for each sample.
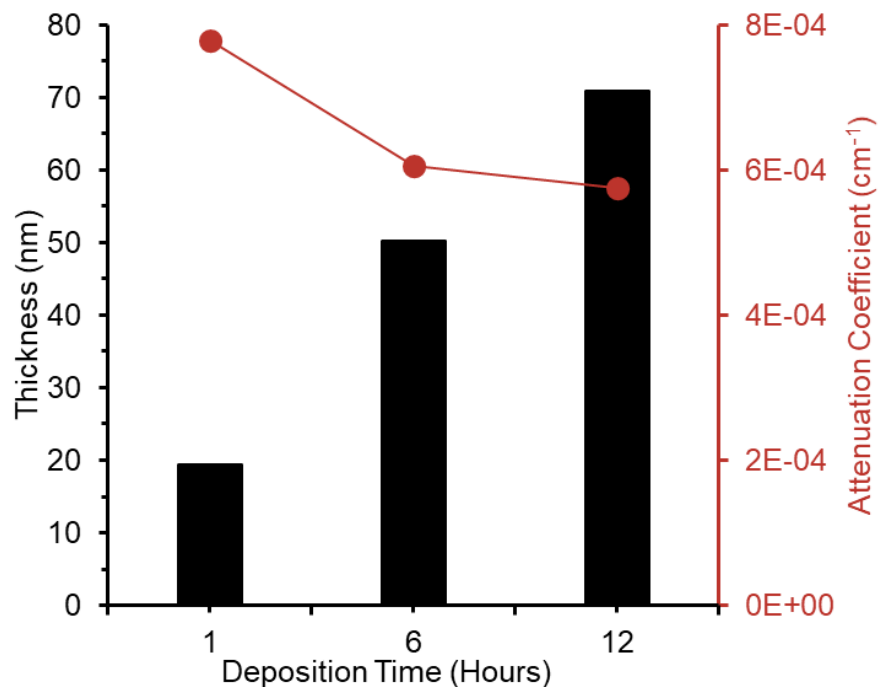
Figure 22. Effect of Deposition Time on Thickness and Attenuation Coefficient at 450 Nanometers.
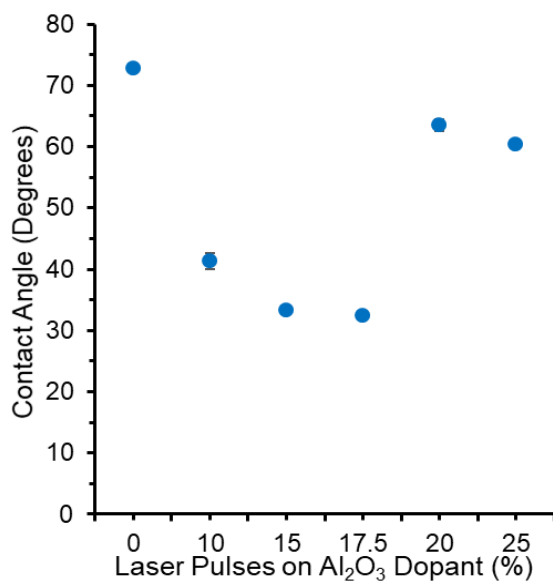
Figure 23. The Effect of Aluminum Oxide Dopant on Average Water Contact Angle. Note: Error Bars are Present but Difficult to Observe for Each Sample.
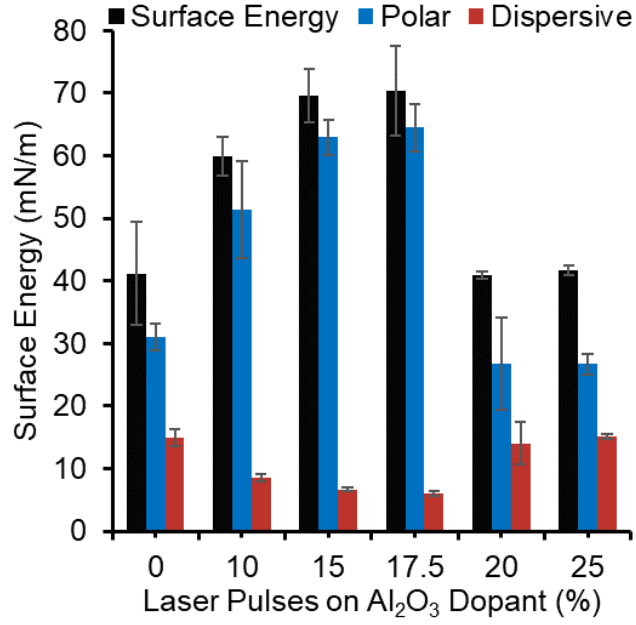
Figure 24. The Effect of Aluminum Oxide Dopant on Average Surface Energy.
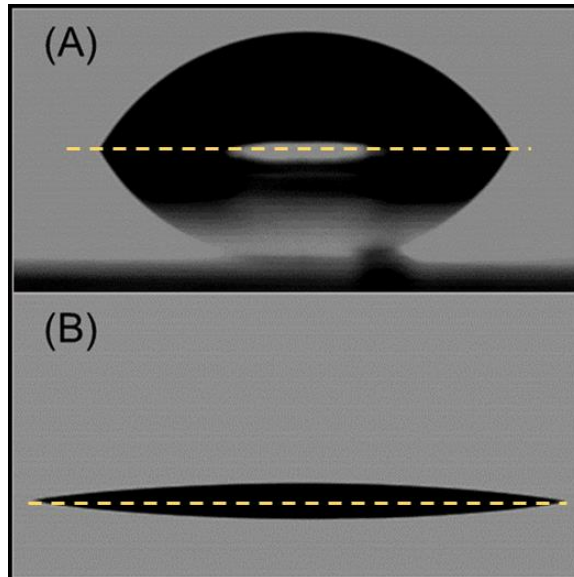
Figure 25. Profile of Water Droplets on 17.5% Aluminum Oxide Doped Samples: (A) an As-Made Film and (B) a Plasma Cleaned Film, Imaged 60 Minutes After Treatment. Note: The baseline for each measurement is indicated with a yellow, dashed line.
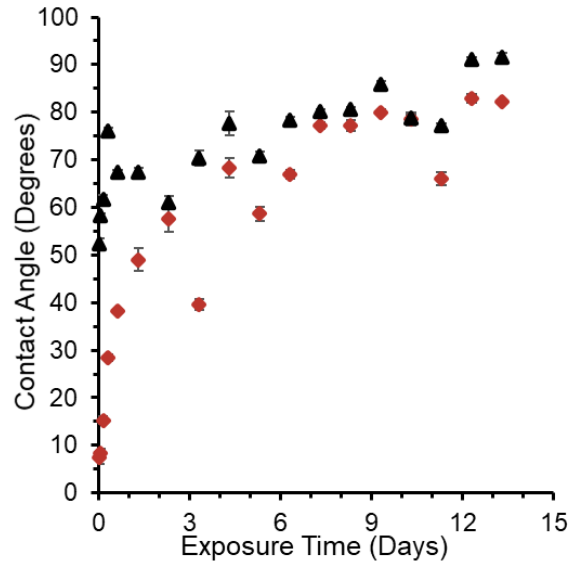
Figure 26. Results of Average Contact Angle Measurements of Plasma Cleaned vs. As-Made 17.5% Films over 14 Days: (A) As-Made; (B) Argon Plasma Cleaned. Note: Error bars are present but difficult to observe for each sample.
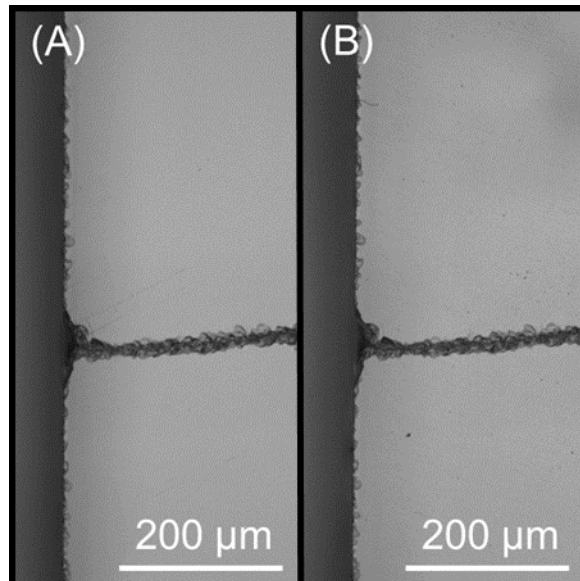
Figure 27. Results of Simulated Body Fluid Soaks for a 10% Al$_2$O$_3$ Doped DLC Film: (A) Before Soaking and (B) After Forty weeks of Soaking.
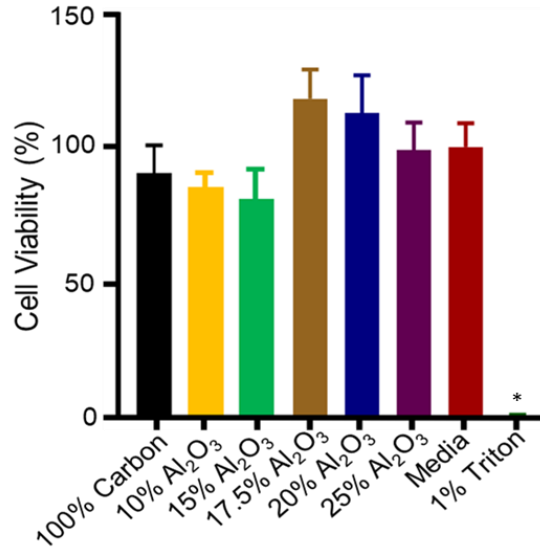
Figure 28. Average Viability Normalized to Media Controls of NIH 3T3 Cells Incubated for 24 Hours with Various Aluminum Oxide Doped DLC Films (n = 5 technical replicates). The significance of the data was evaluated via ordinary one-way ANOVA with Dunnett's Multiple Comparison Test (*$p < 0.05$).
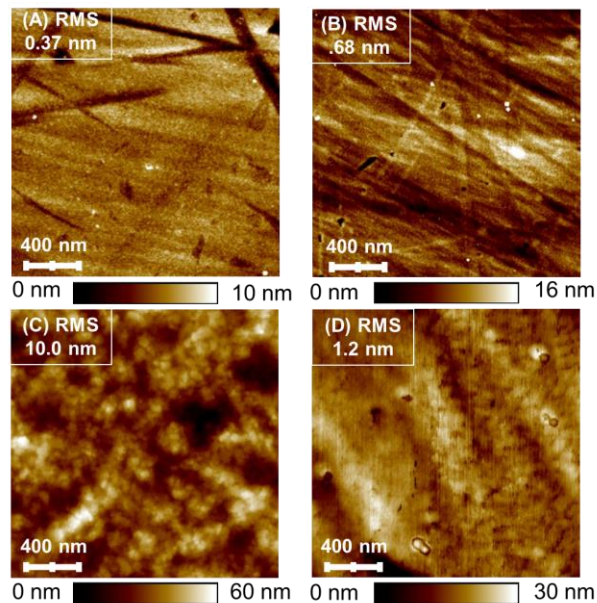
Figure 29. AFM Results of Aluminum Oxide Doped Films: (A) Uncoated substrate, (B) 0% Dopant, (C) 17.5% Dopant, and (D) Plasma Cleaned 17.5% Dopant.
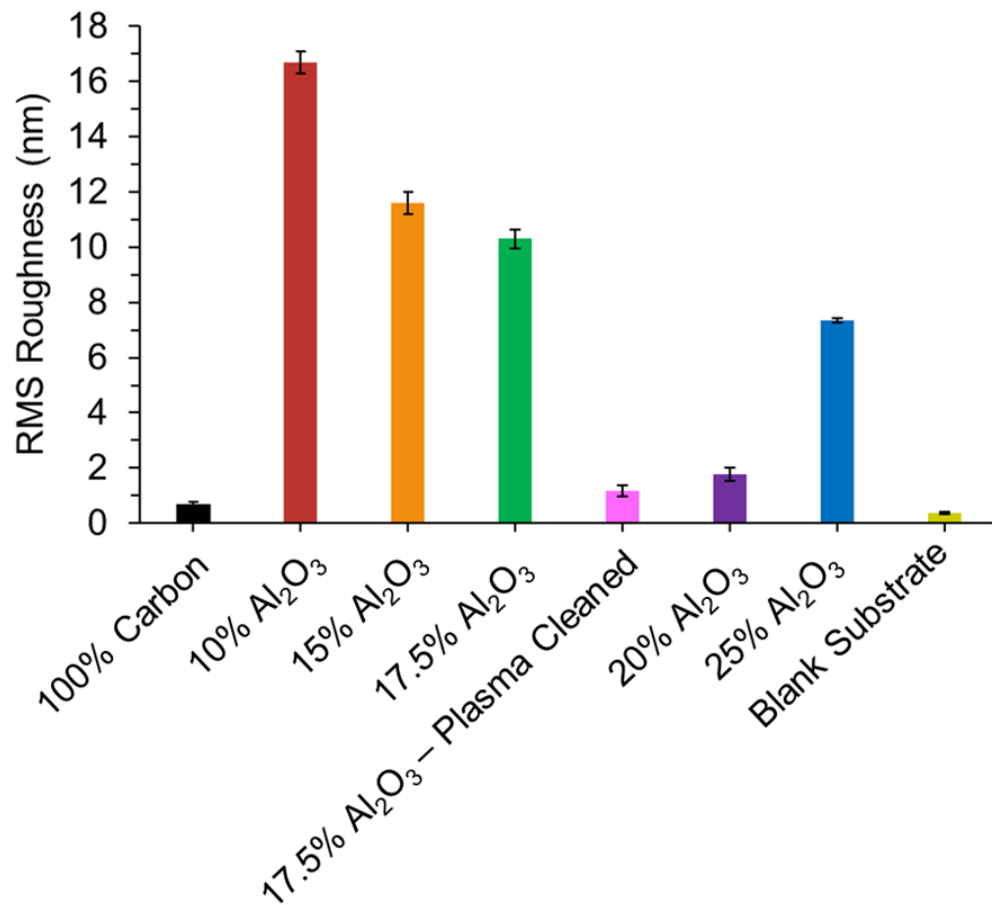
Figure 30. Root Mean Square Roughness of Aluminum Oxide Doped Films Derived from AFM.
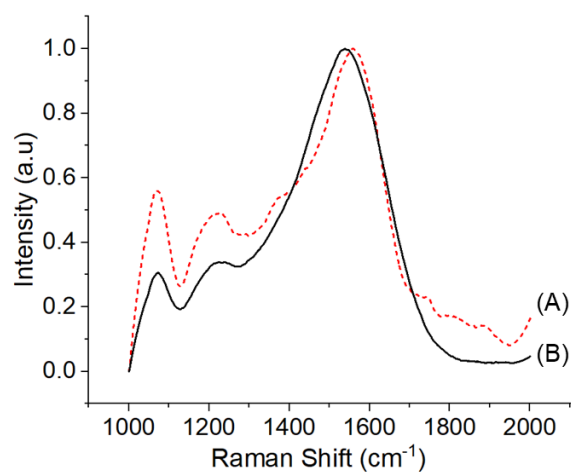
Figure 31. Raman Spectra of DLC Films with Varying Amount of Dopant: (A) 10% Al$_2$O$_3$; (B) 100% Carbon. Note: This data has been normalized.

Table 6. Gaussian Function Fittings of the Raman Spectra for an Undoped and an Aluminum Oxide Doped DLC Film.

Sample Name	Pulses on Dopant (%)	G Peak Position	I_D/I_G	Full Width Half Maximum G Peak
ABB025	None	1548 ± 1	0.41 ± 0.02	266 ± 3
ABB019	10	1571 ± 3	0.57 ± 0.01	198 ± 9

Conclusion

Aluminum oxide doped diamond-like carbon thin films were synthesized by pulsed laser deposition. The goal of this research was to determine if Al_2O_3 was a suitable dopant for DLC to create a transparent, antifogging film for laparoscopes. The doped films demonstrated exceptional transparency over the visible spectrum achieving up to an average of 98% transmission. Additionally, doping the films increased the hydrophilicity and surface energy of DLC at lower dopant amounts. Introduction of Al_2O_3 into the DLC films resulted in the contact angle reducing to 33° at its lowest and surface energy increasing up to 70 mN/m. Plasma cleaning was performed to determine if the hydrophilicity of the films could be further improved. Contact angles after plasma cleaning treatments were reduced to 8°; however, time-studies demonstrated that the effects of this method of surface treatment are short-lived and diminish rapidly within a few hours. CellTiter-Glo assays and simulated body fluid soaks demonstrated the biocompatibility and biostability of the films, respectively. These films are not suitable for antifogging applications because of their relatively high contact angles, which do not show long-term improvements after plasma cleaning treatments. However, because of the satisfactory initial biocompatibility and biostability results, they do show promise for biomedical applications where a transparent coating is necessary. Wear testing and blood biocompatibility characterization of these films in the future could help verify other potential uses for biomedical devices.

CONCLUSION

Diamond-like carbon thin films were effectively synthesized using pulsed laser deposition. SiO and Al_2O_3 were utilized as dopants to improve the transparency and hydrophilic qualities of DLC. Both series demonstrated similar biostability, biocompatibility, and adhesion results with no film failure observed during these tests. The SiO series exhibited greater hydrophilicity, while the Al_2O_3 series was more transparent. The introduction of SiO into the films resulted in contact angles under 40°. Al_2O_3 doped films achieved contact angles under 40° as well, but not across all doping levels. Argon plasma cleaning treatments of SiO and Al_2O_3 doped films resulted in contact angles of less than 5° and 8° respectively within 60 minutes of treatment. The contact angle remained under 20° for three days after treatment for the SiO films, while the Al_2O_3 doped films demonstrated considerably poorer longevity for the contact angle reduction; the contact angle for the Al_2O_3 doped films rose to above 30° on the first day of treatment. Plasma cleaning shows promise for the SiO series as a method of pre-treatment for further reducing contact angles. The cellular viability results for both series were statistically similar to the control media demonstrating the biocompatibility of the films.

As laparoscopic procedures continue to increase in frequency, the development of a solution for intraoperative fogging becomes more important. The results of this research show promise for utilizing doped DLC films as an antifogging coating for laparoscopic lenses. Of the two dopants used, SiO shows more promise as an antifogging coating; however, a DLC film combining the two dopants could be the answer for improved transparency and hydrophilicity. A film with Al_2O_3 doped DLC as the base layer and SiO doped DLC as the top layer could provide better transparency without sacrificing the hydrophilicity of the films surface. Optimizing the level of dopant for maximum transparency and hydrophilicity could lead to these doped DLC films becoming a competitive method of fog reduction in laparoscopic procedures.

REFERENCES

1. Bogdanowicz, R., *Chapter 8 - Advancements in Diamond-Like Carbon Coatings*, in *Handbook of Nanoceramic and Nanocomposite Coatings and Materials*, A.S.H. Makhlouf and D. Scharnweber, Editors. 2015, Butterworth-Heinemann. p. 183-205.
2. Robertson, J., *Diamond-like amorphous carbon.* Materials Science and Engineering: R: Reports, 2002. **37**(4): p. 129-281.
3. Zhang, T.F., et al., *Microstructure and high-temperature tribological properties of Si-doped hydrogenated diamond-like carbon films.* Applied Surface Science, 2018. **435**: p. 963-973.
4. Hilbert, J., et al., *Si doping enhances the thermal stability of diamond-like carbon through reductions in carbon-carbon bond length disorder.* Carbon, 2018. **131**: p. 72-78.
5. Kong, C., et al., *Tribological mechanism of diamond-like carbon films induced by Ti/Al co-doping.* Surface and Coatings Technology, 2018. **342**: p. 167-177.
6. Sánchez-López, J.C. and A. Fernández, *Doping and Alloying Effects on DLC Coatings*, in *Tribology of Diamond-Like Carbon Films: Fundamentals and Applications*, C. Donnet and A. Erdemir, Editors. 2008, Springer US: Boston, MA. p. 311-338.
7. Takai, O., *Chapter 34 - Super-hard Materials*, in *Carbon Alloys*, E.-i. Yasuda, et al., Editors. 2003, Elsevier Science: Oxford. p. 545-558.
8. Roy, R.K. and K.R. Lee, *Biomedical applications of diamond-like carbon coatings: a review.* J Biomed Mater Res B Appl Biomater, 2007. **83**(1): p. 72-84.
9. De Las Heras, E., et al., *Surface Modification by Plasma-Based Processes.* 2009: p. 343-378.
10. Grill, A., *Diamond-like carbon coatings as biocompatible materials—an overview.* Diamond and Related Materials, 2003. **12**(2): p. 166-170.
11. Onodera, S., et al., *Antibacterial property of F doped DLC film with plasma treatment.* Diamond and Related Materials, 2020. **107**: p. 107835.
12. Leonard, R.L., et al., *Antifog coating for bronchoscope lens.* Surface Engineering, 2012. **28**(6): p. 468-472.
13. Lowndes, D.H., et al., *Synthesis of Novel Thin-Film Materials by Pulsed Laser Deposition.* Science, 1996. **273**(5277): p. 898.
14. Krebs, H.-U., et al., *Pulsed Laser Deposition (PLD) -- A Versatile Thin Film Technique.* 2003. p. 101-107.
15. Schneemeyer, L.F., *Crystal Growth*, in *Encyclopedia of Physical Science and Technology (Third Edition)*, R.A. Meyers, Editor. 2003, Academic Press: New York. p. 79-89.
16. Dubček, P., et al., *Texture of GaAs Nanoparticles Deposited by Pulsed Laser Ablation in Different Atmospheres.* ISRN Nanomaterials, 2013. **2013**: p. 576506.
17. Boffoué, M.O., et al., *Pulsed laser deposition of bismuth in the presence of different ambient atmospheres.* Thin Solid Films, 1998. **322**(1): p. 132-137.
18. Nguyen, V.X., V.T. Le Nguyen, and C.C. Nguyen, *Appropriate use of endoscopy in the diagnosis and treatment of gastrointestinal diseases: up-to-date indications for primary care providers.* Int J Gen Med, 2010. **3**: p. 345-57.
19. Dua, A., et al., *National Trends in the Adoption of Laparoscopic Cholecystectomy over 7 Years in the United States and Impact of Laparoscopic Approaches Stratified by Age.* Minimally Invasive Surgery, 2014. **2014**: p. 635461.
20. Drysch, A., et al., *Comparative analysis of techniques to prevent laparoscopic fogging.* Minimally Invasive Therapy & Allied Technologies, 2016. **25**(6): p. 319-322.
21. Richards, C., et al., *Does using a laparoscopic approach to cholecystectomy decrease the risk of surgical site infection?* Annals of surgery, 2003. **237**(3): p. 358-362.
22. Romy, S., et al., *Laparoscope use and surgical site infections in digestive surgery.* Ann Surg, 2008. **247**(4): p. 627-32.
23. Sasmal, P.K., et al., *Port site infection in laparoscopic surgery: A review of its management.* World journal of clinical cases, 2015. **3**(10): p. 864-871.

24. Lawrentschuk, N., N.E. Fleshner, and D.M. Bolton, *Laparoscopic lens fogging: a review of etiology and methods to maintain a clear visual field.* J Endourol, 2010. **24**(6): p. 905-13.

25. Manning, T.G., et al., *Visual Occlusion During Minimally Invasive Surgery: A Contemporary Review of Methods to Reduce Laparoscopic and Robotic Lens Fogging and Other Sources of Optical Loss.* J Endourol, 2017. **31**(4): p. 327-333.

26. Pierson, H.O., *Handbook of carbon, graphite, diamond, and fullerenes : properties, processing, and applications.* 1993, Park Ridge, N.J., U.S.A.: Noyes Publications.

27. Silva, S.R.P. and Inspec, *Properties of amorphous carbon.* 2003, London: INSPEC.

28. Panzer, J., *Components of solid surface free energy from wetting measurements.* Journal of Colloid and Interface Science, 1973. **44**(1): p. 142-161.

29. Fernández, V. and M. Khayet, *Evaluation of the surface free energy of plant surfaces: toward standardizing the procedure.* Frontiers in plant science, 2015. **6**: p. 510-510.

30. Cho, S.-B., et al., *Dependence of Apatite Formation on Silica Gel on Its Structure: Effect of Heat Treatment.* Journal of the American Ceramic Society, 2005. **78**: p. 1769-1774.

31. Nama Manjunatha, K. and S. Paul, *Investigation of optical properties of nickel oxide thin films deposited on different substrates.* Applied Surface Science, 2015. **352**: p. 10-15.

32. *Silicon Monoxide*, in *SDS*. 2015, Kurt J. Lesker Company. p. 8.

33. Baxter, H., et al., *Surgical Instrument Decontamination: Efficacy of Introducing an Argon:Oxygen RF Gas-Plasma Cleaning Step as Part of the Cleaning Cycle for Stainless Steel Instruments.* Plasma Science, IEEE Transactions on, 2006. **34**: p. 1337-1344.

34. Subedi, D., et al., *Retracted: Study of the wettability of ZnO nanofilms.* International Nano Letters, 2012. **2**.

35. Yi, J.W., et al., *Long-Lasting Hydrophilicity on Nanostructured Si-Incorporated Diamond-Like Carbon Films.* Langmuir, 2010. **26**(22): p. 17203-17209.

36. Tarrant, R.N., O. Warschkow, and D.R. McKenzie, *Raman spectra of partially oriented sp2 carbon films: Experimental and modelled.* Vibrational Spectroscopy, 2006. **41**(2): p. 232-239.

37. Ferrari, A.C., *Determination of bonding in diamond-like carbon by Raman spectroscopy.* Diamond and Related Materials, 2002. **11**(3): p. 1053-1061.

38. Little, D., et al., *Femtosecond Laser Modification of Fused Silica: The Effect of Writing Polarization on Si-O Ring Structure.* Optics express, 2008. **16**: p. 20029-37.

39. Yadav, A.K. and P. Singh, *A Review on Structure of Glasses by Raman Spectroscopy.* RSC Advances, 2015. **5**: p. 67583-67609.

40. Spaner, S.J. and G.L. Warnock, *A brief history of endoscopy, laparoscopy, and laparoscopic surgery.* J Laparoendosc Adv Surg Tech A, 1997. **7**(6): p. 369-73.

41. Li, Z. and P.W. Chiu, *Robotic Endoscopy.* Visc Med, 2018. **34**(1): p. 45-51.

42. Sheetz, K.H., J. Claflin, and J.B. Dimick, *Trends in the Adoption of Robotic Surgery for Common Surgical Procedures.* JAMA Network Open, 2020. **3**(1): p. e1918911-e1918911.

43. Ohtake, N., et al., *Properties and Classification of Diamond-Like Carbon Films.* Materials (Basel), 2021. **14**(2).

44. Zhang, M., et al., *Mechanical Properties and Biocompatibility of Ti-doped Diamond-like Carbon Films.* ACS Omega, 2020. **5**(36): p. 22772-22777.

45. Houska, J., et al., *Overview of optical properties of Al2O3 films prepared by various techniques.* Thin Solid Films, 2012. **520**(16): p. 5405-5408.

46. Hannouche, D., et al., *Ceramics in Total Hip Replacement.* 2005. **430**: p. 62-71.

47. Litvinov, J., et al., *Development of pinhole-free amorphous aluminum oxide protective layers for biomedical device applications.* Surface and Coatings Technology, 2013. **224**: p. 101-108.

48.   Nduni, M.N., A.M. Osano, and B. Chaka, *Synthesis and characterization of aluminium oxide nanoparticles from waste aluminium foil and potential application in aluminium-ion cell.* Cleaner Engineering and Technology, 2021: p. 100108.

49.   Wang, S.F., et al., *Transparent ceramics: Processing, materials and applications.* Progress in Solid State Chemistry, 2013. **41**(1): p. 20-54.

50.   Li, Y., et al., *Preparation of Aluminum Nanomesh Thin Films from an Anodic Aluminum Oxide Template as Transparent Conductive Electrodes.* Scientific Reports, 2016. **6**(1): p. 20114.

51.   Wang, J., et al., *Improving frictional properties of DLC films by surface energy manipulation.* RSC Advances, 2018. **8**(21): p. 11388-11394.

52.   Larkin, P.J., *Chapter 6 - IR and Raman Spectra–Structure Correlations: Characteristic Group Frequencies*, in *Infrared and Raman Spectroscopy (Second Edition)*, P.J. Larkin, Editor. 2018, Elsevier. p. 85-134.

APPENDIX
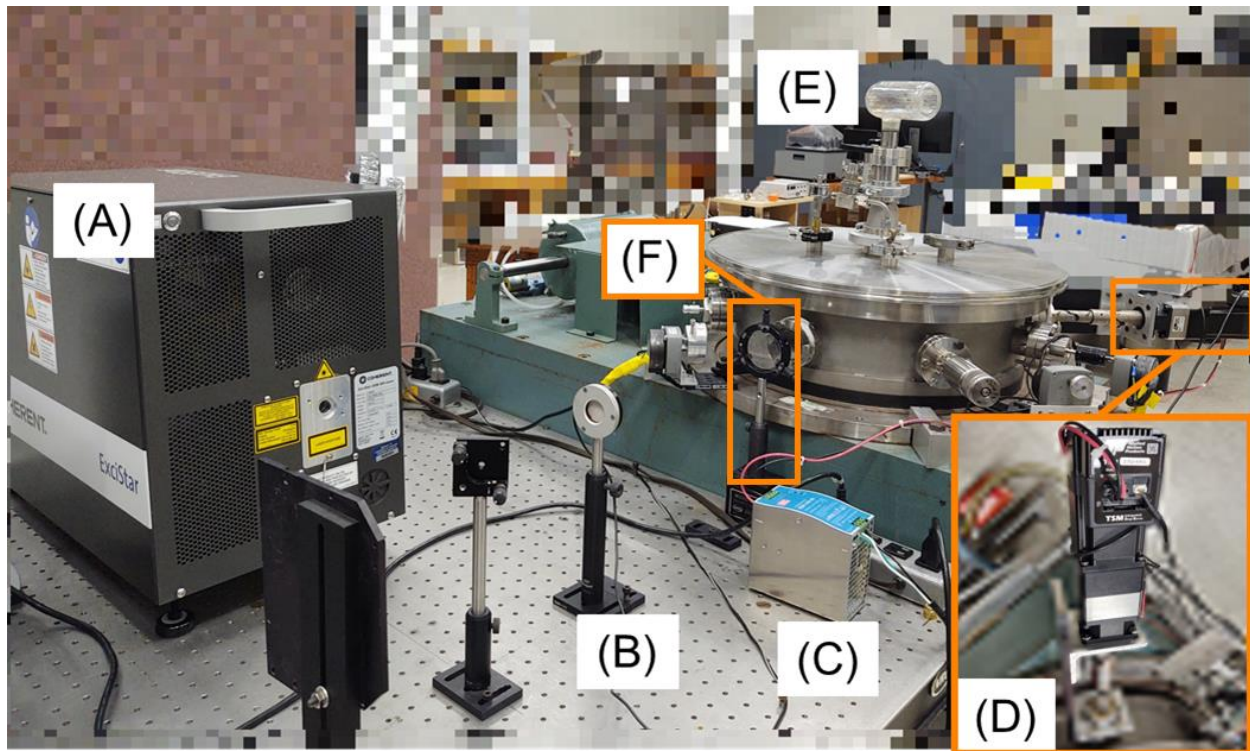
Figure A1. Pulsed Laser Deposition System at UTSI: (A) 193 nm ArF Excimer Laser, (B) Laser Energy Meter, (C) Power Supply for Stepper Motor, (D) Programmable Stepper Motor for Axial Target Rotation, (E) Ion Gauge, and (F) Focusing Lens.

VITA

Anna Beatrice Bull was born in Pleasanton, California to Nathan and Kavann Bull. She has an older brother, Aavery, and a younger sister, Adrienne. She was raised in Dallas, Texas and graduated high school in 2014. She graduated from Collin County Community College with an Associates of Science Degree in Engineering in 2017. In 2019 she earned a Bachelor of Science Degree in Biomedical Engineering from the University of Texas at Dallas. She accepted a graduate research assistantship position at the University of Tennessee Space Institute under Dr. Jacqueline Johnson and received a Master of Science degree in Biomedical Engineering in the fall of 2021. She plans to remain in the BEAMS group at the University of Tennessee Space Institute to continue working towards a PhD.